CHARACTERIZATION OF ERBIUM DOPED FIBERS

by

MAHAN MOVASSAGHI

B.Sc. in Electrical Engineering (Electronics), Amir-Kabir University of Technology, Tehran, Iran, 1992

A THESIS SUBMITTED IN PARTIAL FULFILMENT OF

THE REQUIREMENTS FOR THE DEGREE OF

MASTER OF APPLIED SCIENCE

in

THE FACULTY OF GRADUATE STUDIES

(The Department of Electrical Engineering)

We accept this thesis as conforming

to the required standard

THE UNIVERSITY OF BRITISH COLUMBIA

May 1996

In presenting this thesis in partial fulfillment of the requirements for an advanced degree at the University of British Columbia, I agree that the Library shall make it freely available for reference and study. I further agree that permission for extensive copying of this thesis for scholarly purposes may be granted by the head of my department or by his or her representatives. It is understood that copying or publication of this thesis for financial gain shall not be allowed without my permission.

Department of Electrical Engineering
The university of British Columbia
Vancouver, Canada

Date May 29, 1996

ABSTRACT

In this thesis the theory of operation of single-mode erbium-doped fiber amplifiers pumped at 980 *nm* is described. Details of the derivation of the general rate equation for the propagation of signal, pump, and amplified spontaneous emission are provided. Based on this equation, and McCumber's theory of phonon-terminated optical masers, two closed form expressions are derived. In one of them, the fluorescence spectrum of an erbium-doped fiber is related to its spectral absorption coefficient. Based on this expression, a rigorous basis for the assessment of the applicability of McCumber's theory to the study of ${}^4I_{13/2} \Leftrightarrow {}^4I_{15/2}$ transitions in erbium-doped fibers has been established. For the cases of five silica-based erbium-doped fibers, experiments were performed and the results were used to validate this expression. Another important benefit of this expression is that it does not require a measurement of silica-based fiber's fluorescence spectrum, as it can be simply calculated from the spectral absorption coefficient, simplifying fiber characterization. The other closed form expression, provides a simple means for calculating absorption and emission cross-sections of erbium-doped fibers using the easily measured spectral absorption coefficient, the gain coefficient at one particular wavelength, and the fluorescence lifetime. Also, based on this expression, an analytical method for the simple determination of the erbium ion concentration inside the fiber core is proposed.

Experiments were performed to evaluate the cross-sections of an erbium-doped fiber over the wavelength range 1400-1650 *nm*. To check the accuracy of the calculated cross-sections,

saturation powers at the wavelengths 1530 *nm* and 1550 *nm* were measured and results compared with the ones calculated from the cross-sections, obtaining agreements within 6%.

Problems and difficulties associated with the conventional techniques for the measurement of the spectral fluorescence and of the fluorescence lifetime are described. Also new experimental setups were designed to simplify the measurement of these parameters. Furthermore, experimental techniques for the measurement of other fiber parameters such as, spectral absorption coefficient, gain coefficient, and signal saturation power are described.

The new theoretical and experimental techniques presented in this thesis can provide a much simpler and more accurate means for characterizing erbium-doped fibers, improving the accuracy of the numerical models commonly used for modeling erbium-doped fiber amplifiers.

Table of Contents

List of Tables

List of Figures

Acknowledgments

My deepest gratitude goes to the members of my family for their encouragement and support throughout my education, including the course of this work.

I would like to express my gratitude to Dr. P. Vella, of the National Optics Institute (NOI), for suggesting this project and providing continuous support throughout the course of this work. I also would like to thank Dr. N. A. F. Jaeger for his continual support and guidance during my research.

My gratitude extends to Yves Lacroix, research associate at the NOI, for his invaluable help with the experimental measurements, and for many productive discussions and suggestions. I am also grateful to Lisheng Huang, Dr. F. Chenard, Andre Croteau, Francois Gregoire, and Fernand Sylvain, all at the NOI, who have helped me in various ways throughout the course of this work. I also would like to thank Dr. M. K. Jackson for many fruitful discussions as well as Dr. D. L. Pulfrey and Dr. L. M. Wedepohl for their guidance and invaluable advice during my time at UBC.

I would like to specially thank my friend, Shahram Tafazoli, for his help in computer programming and his invaluable support during my research. Finally, my appreciation goes to all those individuals at the National Optics Institute and the Department of Electrical Engineering who have helped me in numerous ways.

Chapter 1

Introduction

The field of optical fiber communications was introduced less than 20 years ago, when the first light-wave communications system operating near $0.8\mu m$, at a bit rate up to 2.3 *Mbit/s*, and electronic repeaters spaced at about 32 *km*, was demonstrated in 1978 [1]. Since then, one of the major research activities within the area of optical communications has focused on reducing the attenuation in the signal path between the transmitter and the receiver, as well as reducing pulse dispersion. In the mid 1980s, the dispersion problem was overcome by using laser sources with ultra-narrow linewidths and dispersion-shifted fibers [2]. However, the real limitation has been the need to regenerate optical signals, typically every 70-100 *km*, as they undergo attenuation when propagating along a fiber link. The signal regeneration has been traditionally performed using electronic repeaters in which the optical signal is converted into an electric current by a photodiode; the electric current is then amplified and converted back into an optical signal by a laser diode. The electronic speed of such repeaters is fixed once and for all; this limits the information rate of such lightwave systems. Other disadvantages of electronic repeaters are their high cost and complexity, especially for multi-channel lightwave systems, as many parallel repeaters are needed to regenerate several optical channels in the same fiber.

In 1985, just when many believed that the optical systems had approached their peak per-

formance, a research group at Southampton University in the UK, showed that optical fibers doped with the rare earth erbium can exhibit signal gain at a wavelength near $1.55\mu m$ [3], and could replace electronic repeaters. This realization spread to other laboratories soon after, and by early 1987 the first erbium-doped fiber amplifier (EDFA), for telecommunication applications, was demonstrated [4]. A few years later, several systems with erbium-doped fiber amplifiers, which were capable of communicating information at bit rates of 5 *Gbit/s* over 14,000 *km* long fiber links, were demonstrated [5]; this performance was more than 140 times better than the performance of unrepeatered systems in 1985, which were operating at bit rates of up to 4 *Gbit/s* over distances of around 100 *km* [6]. Such radical improvements, together with the numerous desirable properties of erbium-doped fibers, e.g., high gain, low noise, high power conversion efficiency, high saturation power, polarization insensitivity, broad spectral bandwidth, very low coupling loss, low cost, and immunity to interchannel crosstalk [7], have created a general belief in the great impact that these amplifiers will have in future optical fiber communications systems. Hence, many researchers around the world have placed considerable emphasis on improving the performance of EDFAs using numerical models based on rate and propagation equations [8]-[18]. For these models to be relevant, it is important to characterize the erbium-doped fibers accurately. In this regard, precise measurement of several fiber parameters such as the spectral absorption coefficients, the spectral gain coefficients, the spectral fluorescence, the fluorescence lifetime, the erbium density distribution inside the fiber core, the spectral absorption cross-sections, the spectral emission cross-sections, and saturation powers are particularly important. Among these parameters the absorption and emission cross-sections at signal wavelengths and the erbium density distribution inside the fiber

core are the ones which are very difficult to measure accurately. Regarding the values of cross-sections, discrepancies of up to 50% are reported for the different methods used to determine these parameters (see Appendix C for details) [8], [19]. Recently a new technique was proposed which allows determination of the quotient of cross-sections [20]. Nevertheless, lack of access to an accurate method for determination of the absolute values of cross-sections still exists. Likewise, previous attempts to determine the erbium density distribution inside the fiber core have not been successful (see Appendix C for details). This lack of success is primarily due to the small size of the fiber core. Recently D. Uttamchandani *et. al.* [21] have proposed a technique which allows direct determination of the erbium profile in the fiber core. However, as far as we know, there is no means for the accurate determination of erbium ion concentration inside the fiber core.

In this thesis, a new technique for simple and accurate determination of absorption and emission cross-sections is described. Also, an analytical method for the simple determination of the erbium ion concentration inside the fiber is proposed. The work presented in this thesis was performed at the National Optics Institute (NOI). The work on erbium-doped fiber amplifiers at NOI started in early 1990. Since then, the activity has focused on the fabrication of silica-based erbium-doped fibers. The Institute, with its well-equipped fiber fabrication laboratories, which are known to be among the best in their category worldwide [22], now has a mature technology in the fabrication of a large variety of erbium-doped fibers. In order to predict the behavior of amplifiers made using these erbium-doped fibers, and furthermore to improve the fiber design, establishing accurate models for the EDFAs is of particular importance. The work presented in this thesis concerns itself with the full characterization of

erbium-doped fibers, which is the initial and most important step towards establishing a comprehensive model for EDFAs.

In Chapter 2 of this thesis the theory of operation of erbium-doped fiber amplifiers, pumped at 980 *nm,* is described. A new technique for the simple assessment of the applicability of McCumber's theory (see Appendix C for details) to the study of silica-based erbium-doped fibers, a new method for the simple determination of absorption and emission cross-sections, and a new approach to the evaluation of the erbium ion concentration inside the fiber core are presented. Rate equation analysis of the erbium ion population based on a three level system model is provided in Appendix A. In Appendix B, details of the derivation of the general rate equation for the propagation of signal, pump, and amplified spontaneous emission in single-mode erbium-doped fiber amplifiers are given. In Appendix C, previous attempts at the determination of the absorption and emission cross-sections and the erbium density distribution inside the fiber core are described.

In Chapter 3 details of the experimental procedure for the determination of several erbium-doped fiber parameters such as, spectral absorption coefficient, gain coefficient, and signal saturation power are described. Problems and difficulties associated with the conventional techniques for the measurement of the spectral fluorescence and the fluorescence lifetime are explained. Also details of the new experimental setups which were designed to simplify the measurement of these parameters are described.

Finally, a summary of the work, conclusions, and suggestions for improving the work are given in Chapter 4.

Chapter 2

Theory

2.1. Introduction

An erbium-doped fiber amplifier (EDFA) is a system in which combined characteristics of a single-mode fiber and a laser glass are utilized. Built upon this fact, many researchers, have over the past few years, developed several theoretical models for the study of these fiber amplifiers [9]-[18]. These models are important for predicting the behavior and for optimizing the performance of EDFAs. In these models, knowledge of several fiber parameters is required; among these parameters the absorption and emission cross-sections at signal wavelengths and the erbium density distribution inside the fiber core are the ones which are very difficult to measure accurately (see Appendix C for details). Despite extensive efforts placed on the evaluation of cross-sections by several researchers, relatively large uncertainty still exists throughout the literature regarding their actual values, and discrepancies of up to 50% are reported for the different techniques used to determine these parameters [8], [19]. In fact, accurate determination of cross-sections is recognized to be the most challenging task in characterizing erbium-doped fibers [8]. The traditional approach for the determination of cross-sections is based on the Futchbacher-Ladenberg (FL) relationship [23] (see Appendix C for details). However, in 1991, several researchers reported its failure for the case of erbium-

doped glasses [19],[24], [25] (see Appendix C for details). Alternately, in 1991 Miniscalco and Quimby [19], [26], suggested that McCumber's theory of phonon-terminated optical masers [27] could be used to determine these parameters. However, their attempt to validate this application of McCumber's theory to the case of silica-based erbium-doped fibers was not quite successful (see Appendix C for details). Furthermore, their approach for determining cross-sections is complicated and requires a knowledge of many fiber parameters, some of which are very difficult to obtain accurately, e.g., erbium ion density distribution, and Stark-level energies. Recently H. Zech [20] has proposed a new technique which allows determination of the quotient of cross-sections. Nevertheless, as far as we know, still there is no accurate method for determination of the absolute values of cross-sections. Likewise, measurement of the erbium density distribution inside the fiber core is a challenging task. This is because of the small size of the fiber core. Previous attempts to measure this parameter have not been quite successful and the accuracy of the measurements is estimated to be about 18% [28] (see Section 2.5 and Appendix C for more details). Recently D. Uttamchandani *et. al.* [21] showed that confocal optical microscopy can be used for direct measurement of the erbium profile inside the fiber core. Nevertheless, as far as we know, still there is no means for the accurate determination of erbium ion concentration inside the fiber core.

In this chapter, the theory of operation of erbium-doped fiber amplifiers pumped at 980 *nm* is described. Based on the general rate equation for the propagation of the signal, pump and amplified spontaneous emission, for which details of its derivation are described in Appendix B, and on McCumber's theory of phonon-terminated optical masers, a simple means for determining the spectral absorption and emission cross-sections is presented. Finally, a new

approach to the evaluation of the erbium ion concentration inside the fiber core is described.

2.2. Fundamentals of erbium-doped fiber amplifiers

The basic architecture of an erbium-doped fiber amplifier is illustrated in Figure 2.1. The system includes a pump laser diode (LD), a wavelength selective coupler or combiner (WSC), which is also called a wavelength division multiplexer (WDM), and a length of a single-mode erbium-doped fiber (EDF).

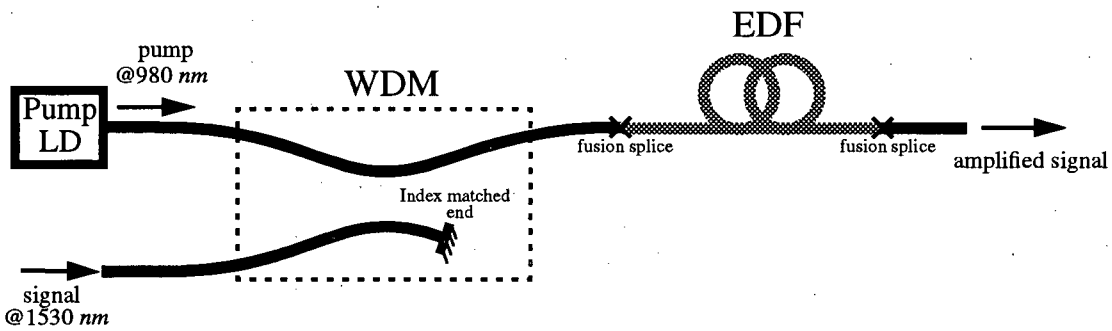

Figure 2.1. Layout of a basic erbium-doped fiber amplifier.

The erbium-doped fiber is made by incorporating erbium dopants together with germania (GeO_2), and/or alumina (Al_2O_3) as co-dopants into the fiber core using various techniques. Among these techniques are, modified chemical vapor deposition (MCVD) [29], [30], vapor axial deposition (VAD) [31], outside vapor deposition (OVD) [32], and solution doping [33].

Alumina and germania are used as index-raising codopants. Furthermore, alumina improves the solubility of the erbium into the fiber core, which results in high concentration doped fibers [34].

The erbium-doped fibers most commonly used are silica-based. The benefits of using silica as the host glass are that it is directly compatible with telecom fibers and hence fusion splicing is possible, yielding ultra low loss and low reflection joints, and that it is an exceptionally durable glass.

The energy levels of erbium ions in silica glasses are shown in figure 2.2. The cross-hatched rectangles in the figure indicate that the main energy levels are split into multiple sub-levels due to the Stark effect. The Stark effect is induced by the permanent electric field, called a crystal or ligand field, which is generated by the charge distribution in the glass host [35].

The transition corresponding to the 1520-1570 *nm* signal band, known as the third telecommunications window, is the one from $^4I_{13/2}$ to $^4I_{15/2}$. The $^4I_{13/2}$ level is the metastable state, and the $^4I_{15/2}$ level, is the ground state. The population inversion between these two levels is achieved by optically pumping the erbium ions from the ground state to some higher state from which the ions relax to the metastable state. Once the population inversion is achieved, signal amplification in the 1520-1570 *nm* band is accomplished by stimulated emission [36].

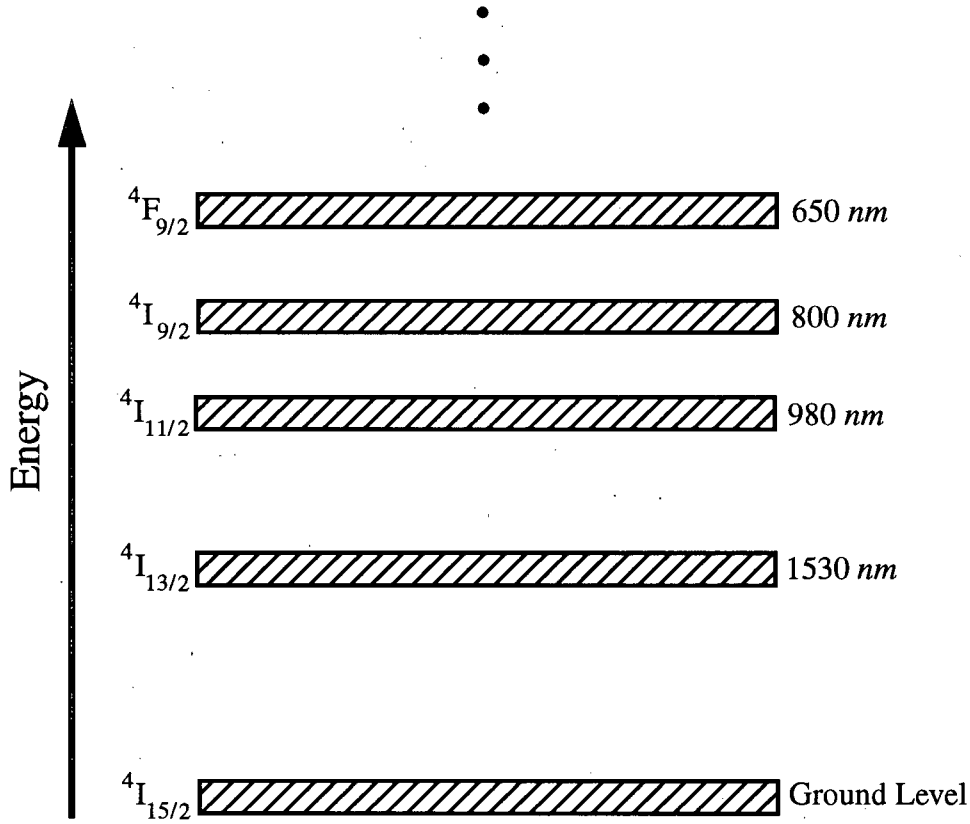

Figure 2.2. Energy levels of erbium ions in a silica glass host.

Among the several transitions that can be used to pump EDFAs, the ${}^4I_{15/2} \rightarrow {}^4I_{11/2}$ transition, which corresponds to the 980 *nm* pump band, offers the highest gain efficiencies [37], [38], and the lowest noise figures [39], [40]. Recent developments in the field of semiconductor lasers has made it possible to make 980 *nm* laser diodes with very high output powers (near 450 *mW*) [41]. Hence, 980 *nm* is currently the preferred pump band and throughout the work presented in this thesis 980 *nm* pumping was used.

To analyze the interactions between the erbium ions and the signal and pump photons in

erbium-doped fiber amplifiers pumped at 980 *nm*, rate equations corresponding to a basic three level laser system have been used throughout the literature. These rate equations are described in Appendix A. Subsequently, in Appendix B, details of the derivation of the general rate equation for the propagation of signal, pump, and amplified spontaneous emission in single-mode EDFAs is provided. In subsequent sections of this chapter, mainly based on this general rate equation, equation (B.21), several closed-form expressions are derived by which a number of difficult-to-measure parameters, e.g., absorption and emission cross-sections at signal wavelengths and the erbium ion concentration in the fiber core, are related to easily measurable parameters.

2.3. Validation of the applicability of McCumber's theory to the study of silica-based erbium-doped fibers - Spectral correlation between fluorescence and absorption coefficient.

Until now, McCumber's theory of phonon-terminated optical masers has been shown to be ideally appropriate for the study of $^4I_{15/2}$ and $^4I_{13/2}$ levels of erbium in glass hosts. However, previous attempts to experimentally verify this application of McCumber's theory have not been successful. This lack of success is primarily due to the fact that the approach taken in those experimental assessments requires knowledge of many fiber parameters which cannot be measured accurately. Essential among these are the erbium ion concentration inside the fiber core and Stark level energies (see Appendix C for details).

In this section, based on McCumber's theory and the general rate equation, equation

(B.21), we derive a closed form expression which relates the fluorescence to the absorption coefficient for the ${}^4I_{13/2} \Leftrightarrow {}^4I_{15/2}$ transitions, the transition of erbium ions from ${}^4I_{13/2}$ level to ${}^4I_{15/2}$ and vice-versa, in erbium-doped glasses. Since in erbium-doped fibers the fluorescence and absorption coefficients can be measured with good accuracy (less than 2% error) [8], comparison of the calculated fluorescence, calculated from the absorption coefficient using our expression, with the measured one provides a reliable means for assessing the applicability of McCumber's theory to the study of these fibers. Finally, using this approach, we validate the applicability of McCumber's theory to the study of ${}^4I_{13/2} \Leftrightarrow {}^4I_{15/2}$ transitions in silica-based erbium-doped fibers.

We start with the general rate equation, equation (B.21). Let us assume that in an amplifier the following conditions are achieved:

1- The pump power is very high, i.e., $\frac{P_p(\lambda_p, z)}{P_{sat}(\lambda_p)} \gg 1$;

2- The signal power at any fiber coordinate z is much lower than the pump power, i.e., $P_s(\lambda, z) \ll P_p(\lambda_p, z)$, and also that $\frac{P_s(\lambda, z)}{P_{sat}(\lambda)} \ll 1$ but is still strong enough such that amplified spontaneous emission can be neglected, i.e., $P_s(\lambda, z) \gg P_{ASE}(\lambda, z)$.

Under these operating conditions, equation (B.21) can be simplified to:

$$\frac{dP_s(\lambda, z)}{dz} = \frac{2}{\omega_s^2(\lambda)} \int_0^\infty \rho(r)\sigma_e(\lambda)P_s(\lambda, z)\psi_s(\lambda, r)r dr \ . \qquad (2.1)$$

where the term $\frac{dP_s(\lambda, z)}{P_s(\lambda, z)dz} = \frac{d[\ln P_s(\lambda, z)]}{dz}$ is defined as the signal gain coefficient $g_s(\lambda)$. Therefore, in terms of $g_s(\lambda)$ equation (2.1) can be written as:

$$g_s(\lambda) = \frac{2}{\omega_s^2(\lambda)} \sigma_e(\lambda) \int_0^\infty \rho(r)\psi_s(\lambda, r) r dr \ . \tag{2.2}$$

On the other hand, let us assume an amplifier in which the pump is turned off, i.e., $P_p(\lambda_p, z) = 0$, and the signal power is so small that $\frac{P_s(\lambda, z)}{P_{sat}(\lambda)} \ll 1$. Under this condition, ASE can be neglected, and equation (B.21) can be simplified to:

$$\frac{dP_s(\lambda, z)}{dz} = -\frac{2}{\omega_s^2(\lambda)} \int_0^\infty \rho(r)\sigma_a(\lambda)P_s(\lambda, z)\psi_s(\lambda, r) r dr \ , \tag{2.3}$$

where the term $-\frac{dP_s(\lambda, z)}{P_s(\lambda, z)dz} = -\frac{d[\ln P_s(\lambda, z)]}{dz}$ is defined as the signal absorption coefficient, $\alpha_s(\lambda)$. In terms of $\alpha_s(\lambda)$, equation (2.3) can be written as:

$$\alpha_s(\lambda) = \frac{2}{\omega_s^2(\lambda)} \sigma_a(\lambda) \int_0^\infty \rho(r)\psi_s(\lambda, r) r dr \ . \tag{2.4}$$

Now, let us consider an amplifier in which the signal is turned off, i.e., $P_s(\lambda, z) = 0$, and the pump power is so high that $\frac{P_p(\lambda_p, z)}{P_{sat}(\lambda_p)} \gg 1$. Under this operating condition, equation (B.21) can be simplified to:

$$\frac{dP_{ASE}(\lambda, z)}{dz} = \frac{4P_0(\lambda)\sigma_e(\lambda)}{\omega_s^2(\lambda)} \int_0^\infty \rho(r)\psi_s(\lambda, r) r dr \ . \tag{2.5}$$

Accordingly, the ASE power of a length L of an erbium-doped fiber at wavelength λ and wavelength interval $\Delta\lambda$ can be obtained by integration of equation (2.5):

$$P_{ASE}(\lambda, L) = \frac{4LP_0(\lambda)\sigma_e(\lambda)}{\omega_s^2(\lambda)} \int_0^\infty \rho(r)\psi_s(\lambda, r) r dr \ . \tag{2.6}$$

The ASE power at low gains, i.e., very short fiber lengths, is the fluorescence $F(\lambda)$ [44]. Thus, from the combination of equations (2.2) and (2.6), we obtain:

$$\frac{F(\lambda)}{g_s(\lambda)} = 2LP_0(\lambda) = \frac{2Lhc^2\Delta\lambda}{\lambda^3} \ , \tag{2.7}$$

which gives a relationship between fluorescence and gain coefficient.

From equations (2.2) and (2.4) the relation

$$\frac{\sigma_e(\lambda)}{\sigma_a(\lambda)} = \frac{g_s(\lambda)}{\alpha_s(\lambda)} \tag{2.8}$$

is easily obtained. Now, from equation (2.8) and the McCumber relation, equation (C.3), we obtain the expression:

$$\varepsilon = \frac{hc}{\lambda} + k_B T \ln\left[\frac{g_s(\lambda)}{\alpha_s(\lambda)}\right] \ . \tag{2.9}$$

Equation (2.9) provides an alternative means for the simple determination of ε, the parameter which is defined in equation (C.4). To evaluate ε, one can simply measure the absorption and gain coefficients at a particular wavelength λ. In order to minimize measurement errors, we choose λ to be at the peak of the absorption spectrum λ_{peak}. This is because, in deriving equation (B.21) the effect of fiber background loss has not been taken into account. Therefore, $\alpha_s(\lambda)$, in equation (2.4), represents only the absorption coefficient due to erbium dopants, and $g_s(\lambda)$, in equation (2.5), represents the gain coefficient, assuming the fiber background

loss is zero. On the other hand, as $\alpha_s(\lambda)$ and $g_s(\lambda)$ cannot be measured directly, instead, the fiber absorption coefficient, $\alpha'_s(\lambda) = \alpha_s(\lambda) + \alpha_b(\lambda)$, and fiber gain coefficient, $g'_s(\lambda) = g_s(\lambda) - \alpha_b(\lambda)$, are measured using the conventional cutback method [43], where $\alpha_b(\lambda)$ is the background loss coefficient of the fiber. Thus, to obtain $\alpha_s(\lambda)$ and $g_s(\lambda)$, $\alpha_b(\lambda)$ has to be determined first. Since the fiber background loss in the spectral range $\lambda = 1400 - 1650\ nm$ is masked by the loss due to erbium dopants, the value of $\alpha_b(\lambda)$ is determined by extrapolating the fiber background loss coefficients measured at wavelengths away from the erbium absorption band [44]. Hence, $\alpha_b(\lambda)$ cannot be determined accurately. However, since values of $\alpha_b(\lambda)$ are very small (typically around 0.06 *dB/m* for silica-based fibers [50]) compared with the values of $\alpha_s(\lambda)$ and $g_s(\lambda)$, the errors introduced by uncertain values of $\alpha_b(\lambda)$ into the calculated values of $\alpha_s(\lambda)$ and $g_s(\lambda)$ are extremely small. Obviously, the errors are minimum at the peak values of $\alpha_s(\lambda)$ and $g_s(\lambda)$, and since the peaks of these two are very close together, around 1 nm apart in silica-based erbium-doped fibers, in equation (2.9) by choosing λ to be at the peak of the absorption spectrum, we can minimize the error in the calculation of ε. Accordingly, equation (2.9) takes the form:

$$\varepsilon = \frac{hc}{\lambda_{peak}} + k_B T \ln\left[\frac{g_s(\lambda_{peak})}{\alpha_s(\lambda_{peak})}\right] . \tag{2.10}$$

Now, from the combination of equations (2.7), (2.8), (2.10), and (C.3), we can write:

$$\frac{F(\lambda)\lambda^3 \Delta\lambda_{peak}}{F(\lambda_{peak})\lambda_{peak}^3 \Delta\lambda} = \frac{\alpha_s(\lambda)}{\alpha_s(\lambda_{peak})} \exp\left(\frac{hc(1/\lambda_{peak} - 1/\lambda)}{k_B T}\right) , \tag{2.11}$$

which provides the correlation between the absorption coefficient and the fluorescence spectrum. Since, in the measurement of the fluorescence spectra, using an optical spectrum ana-

lyzer, the resolution of the instrument can be chosen to be fixed (e.g., $\Delta\lambda = 0.5nm$) over the entire sweep of the fluorescence spectrum, $\Delta\lambda = \Delta\lambda_{peak}$ and equation (2.11) takes the form:

$$\frac{F(\lambda)\lambda^3}{F(\lambda_{peak})\lambda_{peak}^3} = \frac{\alpha_s(\lambda)}{\alpha_s(\lambda_{peak})} \exp\left(\frac{hc(1/\lambda_{peak} - 1/\lambda)}{k_B T}\right). \tag{2.12}$$

To verify equation (2.12) one would first measure the fluorescence and the absorption coefficient spectra. Then, using the measured absorption coefficient spectrum, the fluorescence spectrum would be calculated using equation (2.12). Finally, the calculated and measured fluorescence spectra would be compared. We measured the spectral fluorescence and absorption coefficient of four germano-alumino silicate erbium-doped fibers in the wavelength range 1450-1650 *nm* (details of the experimental procedures for measuring the absorption coefficient and fluorescence are explained in sections 3.2 and 3.3, respectively). These fibers each had a different erbium concentration, see Table 2.1. Figures 2.3 (a)-(d) show the measured absorption and the measured and calculated fluorescence spectra; both fluorescence spectra have been normalized with respect to their values at λ_{peak}. Table 2.1 also gives estimates of the measurement errors (for the case of absorption these were obtained by performing several cutbacks and for the case of fluorescence by performing several measurements on different pieces of fiber). We have also calculated the maximum discrepancy between the calculated and measured fluorescence over the wavelength range of interest, 1520-1560 *nm*, for each fiber. As can be seen in Table 2.1,the peak discrepancies range from a low of 3% to a maximum of 6%.

Table 2.1. Fiber Parameters, estimated errors, and maximum discrepancies in the 1520-1560 *nm* range, for the four fibers, for which the absorption coefficient and normalized fluorescence spectra are given in Fig. 2.3(a)-(d).

Fiber	Peak Absorption (dB/m)	Estimated Fluorescence Meas. Error	Estimated Absorption Meas. Error	Erbium Concentration (ppm-wt)	Max. Discrepancy Between Measured and Calculated Fluorescence in the 1520-1560 nm Range
1	1.45	1.1%	1.7%	450	5.7%
2	5.26	2.0%	0.8%	950	3.1%
3	16.01	2.3%	1.1%	2000	4.8%
4	35.49	2.6%	1.4%	4400	3.2%

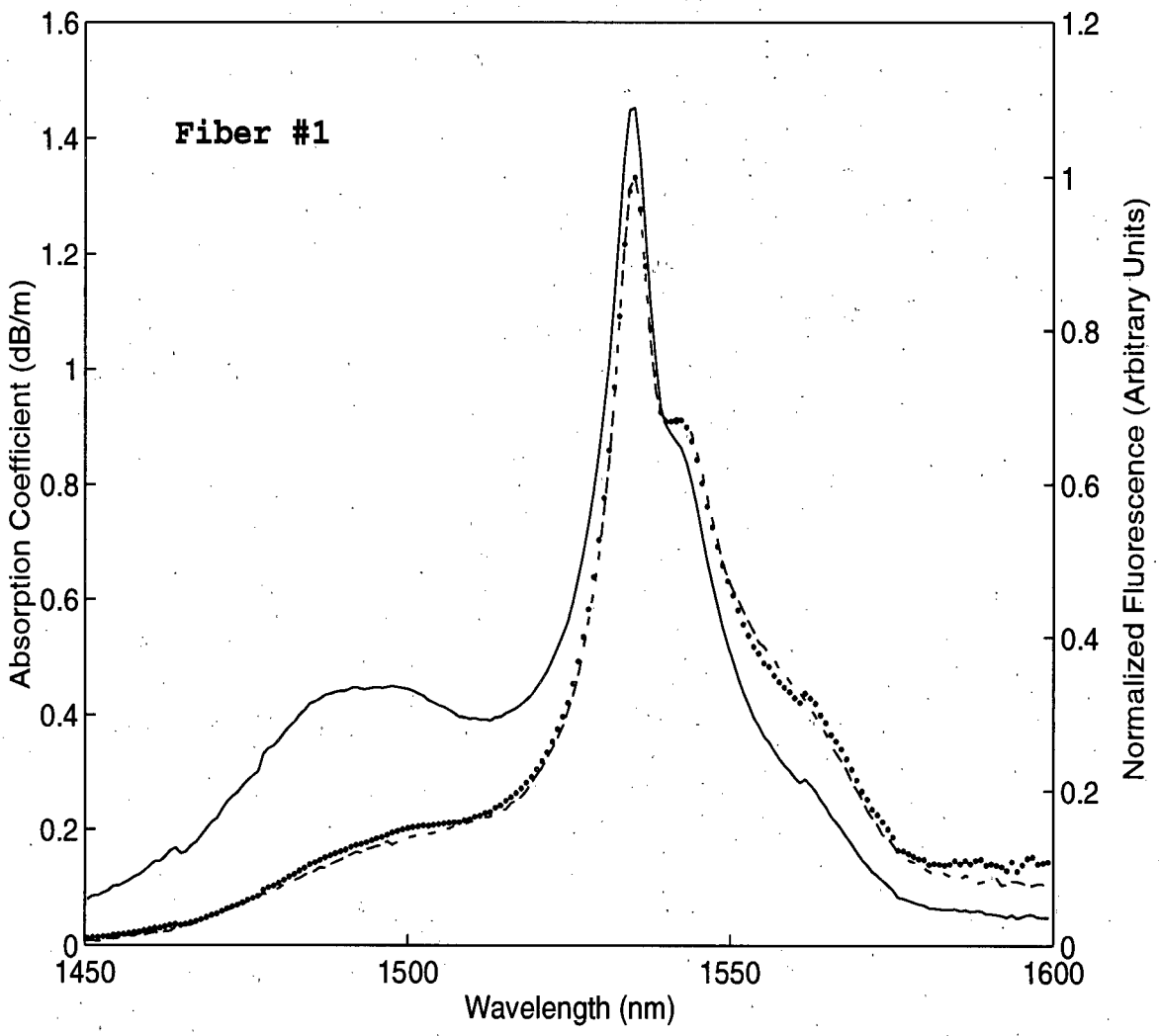

Figure 2.3 (a): Measured absorption coefficient (solid), and the measured (dashed) and calculated (dotted) fluorescence for Fiber #1.

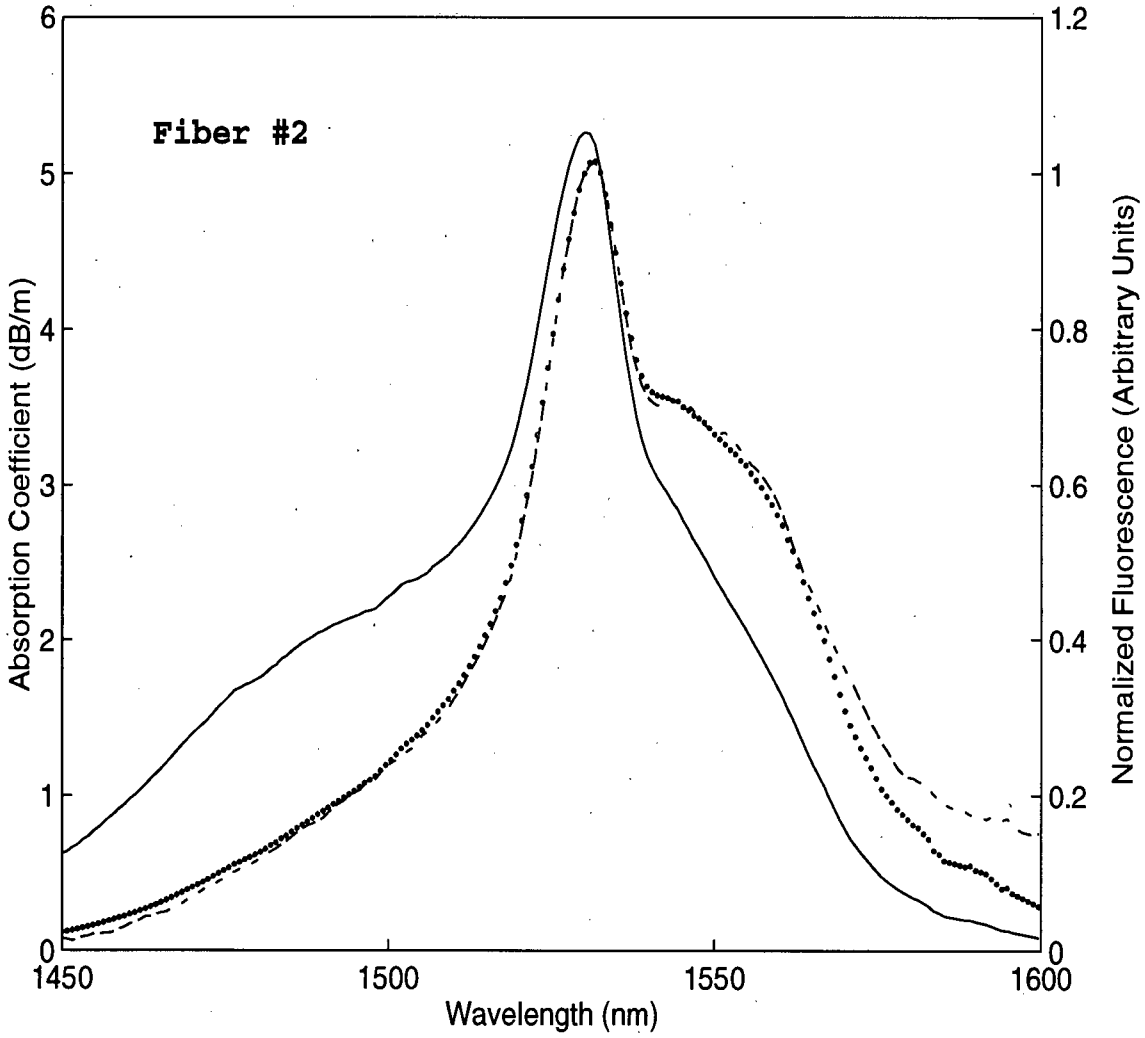

Figure 2.3 (b): Measured absorption coefficient (solid), and the measured (dashed) and calculated (dotted) fluorescence for Fiber #2.

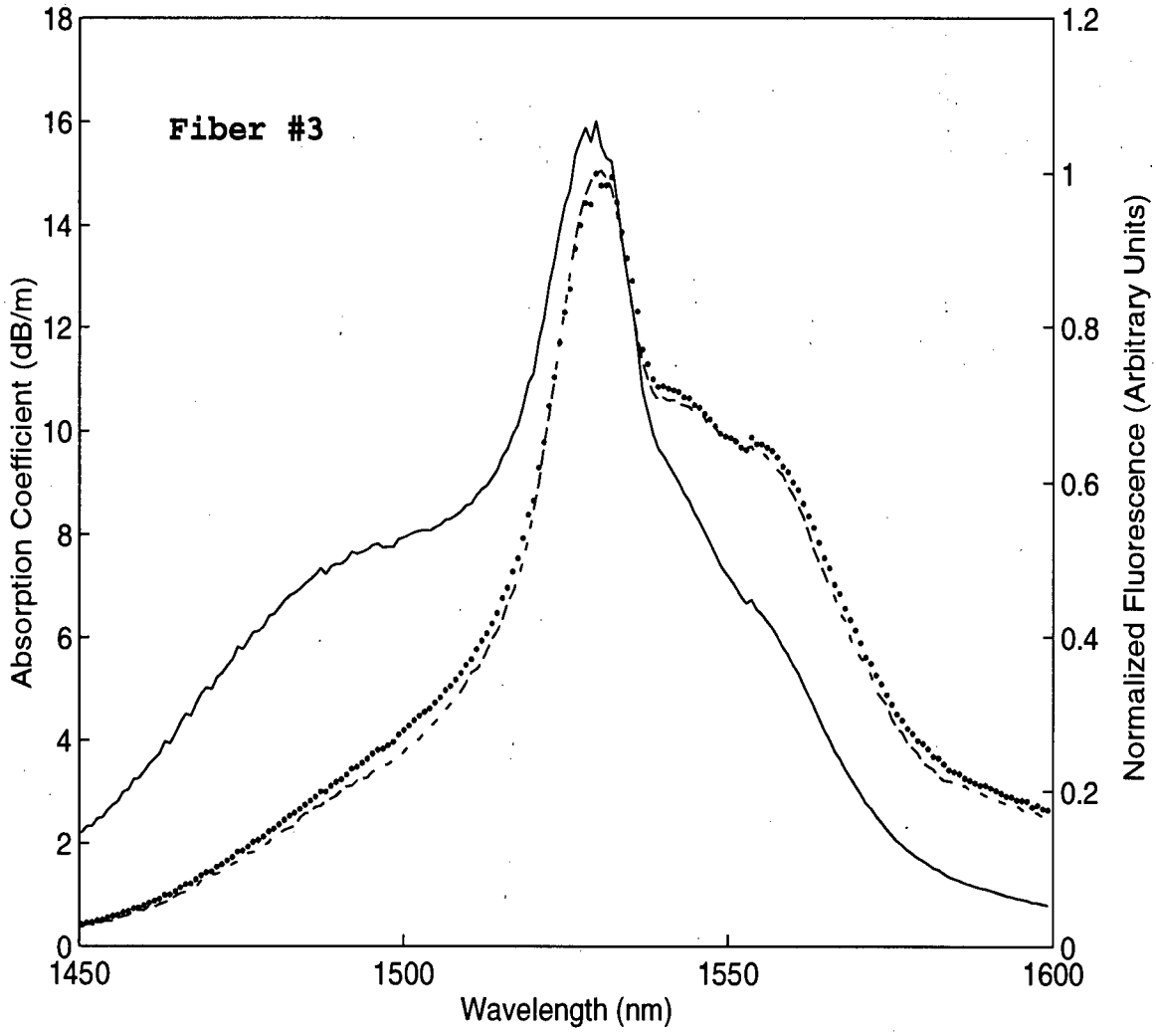

Figure 2.3 (c): Measured absorption coefficient (solid), and the measured (dashed) and calculated (dotted) fluorescence for Fiber #3.

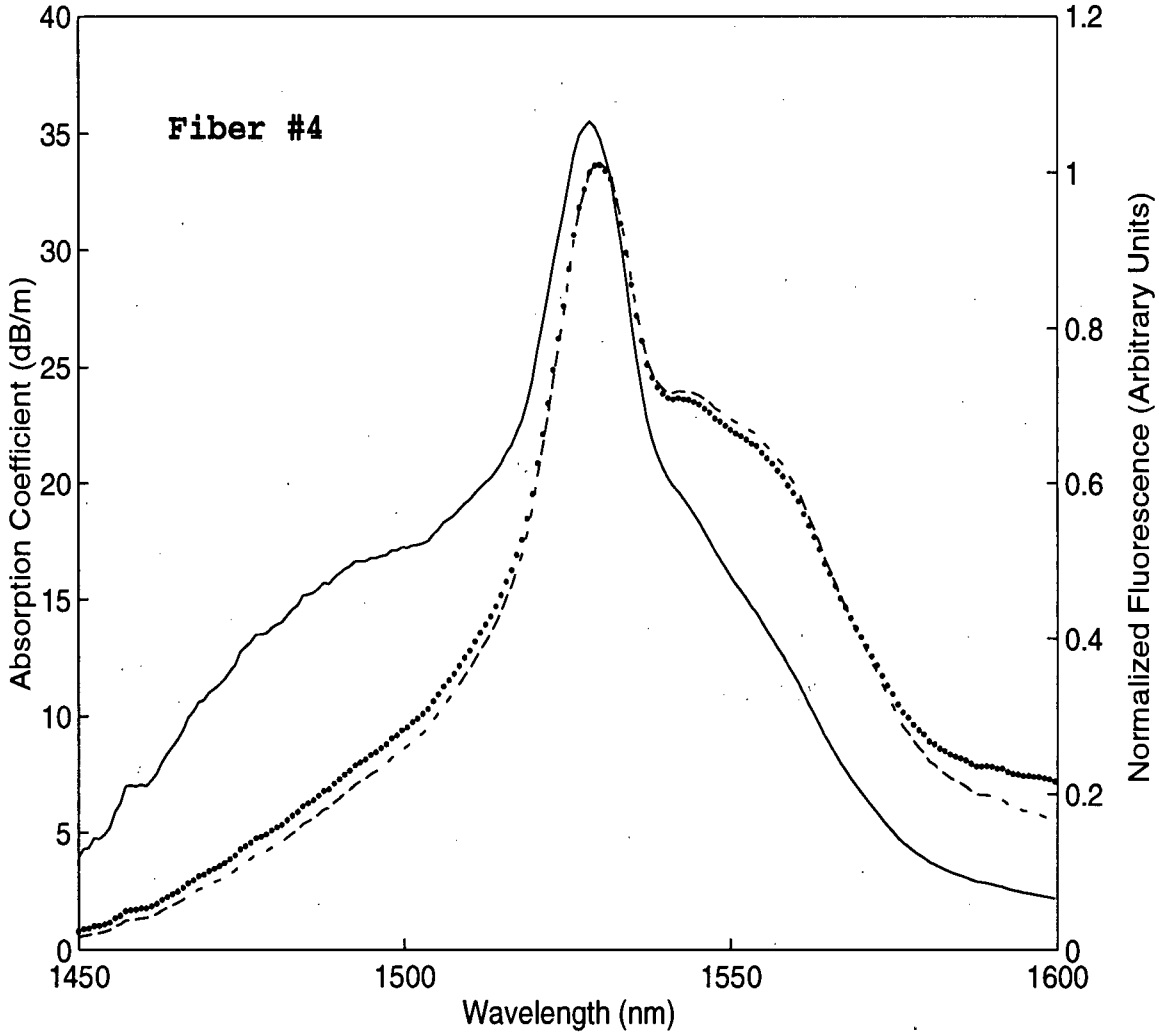

Figure 2.3 (d): Measured absorption coefficient (solid), and the measured (dashed) and calculated (dotted) fluorescence for Fiber #4.

The close agreement between the calculated and measured fluorescence spectra of these fibers validates our closed form expression, equation (2.12), and, thereby, the applicability of McCumber's theory to the study of the ${}^4I_{13/2} \Leftrightarrow {}^4I_{15/2}$ transitions in silica-based erbium-doped fibers. A direct, and important, benefit of our validation of equation (2.12) is that it is no longer necessary to measure a silica-based fiber's fluorescence spectrum when the absorption spectrum is available, as it can be simply calculated. Since both the absorption and fluorescence spectra are among the essential parameters that have to be measured, when characterizing a fiber, our expression provides a simpler means for fiber characterization as the fluorescence measurement can be eliminated.

2.4. A new method for the simple determination of cross-sections

As was discussed in section 2.2, despite extensive efforts directed towards evaluating the absorption and emission cross-sections, relatively large uncertainty is still being expressed in the literature with regard to their actual values. This is primarily due to the fact that the evaluation of these parameters depends on the exact determination of the erbium density distribution within the fiber, which is very difficult to measure accurately.

In this section, a new technique will be presented by which the absorption and emission cross-sections of ${}^4I_{13/2} \Leftrightarrow {}^4I_{15/2}$ transitions can be conveniently and accurately determined using the easily measured spectral absorption coefficient, the gain coefficient at one particular

wavelength, and the fluorescence lifetime. In our technique, based upon McCumber's theory and the general rate equation, equation (B.21), we derive a closed form expression in which we have removed the need to determine the overlap integral, containing the difficult to measure erbium density distribution, by substituting an equivalent expression that contains more easily measured parameters. This vastly simplifies and improves the accuracy of the calculation of the absorption and emission cross-sections.

We start with equation (C.6) from McCumber's theory of phonon-terminated optical masers, which when combined with equation (2.2) gives:

$$\frac{1}{\tau} = 4\pi c n^2 \int_{\lambda_1}^{\lambda_2} \frac{\omega_s^2(\lambda)\, g_s(\lambda)}{\lambda^4 \int_0^{\infty} \rho(r)\psi_s(\lambda, r) r dr} d\lambda \ , \tag{2.13}$$

where λ_1 is at one end of the ${}^4I_{13/2} \rightarrow {}^4I_{15/2}$ emission spectrum and λ_2 is at the other end of the spectrum. Now, from the mean value theorem [45], equation (2.13) can be written as:

$$\int_0^{\infty} \rho(r)\psi_s(\lambda^*, r) r dr = 4\pi\tau c n^2 \int_{\lambda_1}^{\lambda_2} \frac{\omega_s^2(\lambda) g_s(\lambda)}{\lambda^4} d\lambda \ , \tag{2.14}$$

where $\lambda_1 < \lambda^* < \lambda_2$. In equation (2.14) the overlap integral at wavelength λ^*, the mean overlap integral, is expressed in terms of τ, $\omega_s(\lambda)$, and $g_s(\lambda)$. Therefore, in order to evaluate the mean overlap integral, these three parameters have to be determined. The fluorescence lifetime, τ, can be simply measured by monitoring the decaying fluorescence from a length of erbium-doped fiber pumped by a chopped laser beam operating at $\lambda = 980\ nm$. The details

of the experimental procedure are explained in section 3.3. To evaluate the mode power radius, ω_s, we consider the case of a weakly guiding step-index fiber (applicable to the case of commonly used single-mode erbium-doped fibers [46]), for which the fundamental mode is well approximated by the LP_{01} solution [47], [48]. The LP_{01} solution for the fundamental mode envelope is given by [46], [48]:

$$\psi_s(r \le a) = J_0^2\left(\frac{Ur}{a}\right), \tag{2.15}$$

and

$$\psi_s(r > a) = \frac{J_0^2(U)}{K_0^2(W)} K_0^2\left(\frac{Wr}{a}\right),$$

where a is the core radius, J_0 and K_0 are the Bessel and modified Bessel (or Macdonald's) functions, respectively, U and W are the transverse propagation constants of LP_{01} mode, which are given by [47]:

$$U = \frac{(1+\sqrt{2})V}{1+(4+V^4)^{0.25}}, \tag{2.16}$$

and

$$W = (V^2 - U^2)^{\frac{1}{2}},$$

where V is the normalized frequency, and is defined as [47]:

$$V = \frac{2\pi a NA}{\lambda} \tag{2.17}$$

and NA is the fiber numerical aperture given by [48]:

$$NA = (n_{core} - n_{clad})^{\frac{1}{2}}, \tag{2.18}$$

where n_{core} and n_{clad} are the refractive indices of core and cladding, respectively. Now, from the definition of ω_s according to equation (B.9), and by using equation (2.15), ω_s can be written as [8]:

$$\omega_s(\lambda) = a \frac{VK_1(W)}{UK_0(W)} J_0(U) \ . \tag{2.19}$$

Therefore, by knowing the fiber core radius and its numerical aperture, $\omega_s(\lambda)$ can be simply calculated from equation (2.19).

The last parameter in equation (2.14), $g_s(\lambda)$, cannot be measured easily, as it should be determined over the entire ${}^4I_{13/2} \rightarrow {}^4I_{15/2}$ emission spectrum, which is a wide spectral range (typically from 1400-1650 *nm* for the case of silica-based erbium-doped fibers). In order to avoid this, we determined $g_s(\lambda)$, from the fluorescence spectrum and by measuring the gain coefficient at only one particular wavelength, say $g_s(\lambda_x)$, through the relation that is derived earlier in equation (2.7). In other words, equation (2.7) can be written as:

$$\frac{g_s(\lambda)}{g_s(\lambda_x)} = \frac{\lambda^3}{\lambda_x^3} \frac{F(\lambda)}{F(\lambda_x)} \ . \tag{2.20}$$

Giles *et. al.* [44], give a similar, but different, relation between the gain coefficient and the fluorescence, $g_s(\lambda)/g_s(\lambda_x) = F(\lambda)/F(\lambda_x)$, which we believe is not exact.

In equation (2.20), $F(\lambda)/F(\lambda_x)$ can either be determined experimentally, or it can be simply obtained from the measured absorption coefficient spectrum and, using the relation that is derived in equation (2.12), and $g_s(\lambda_x)$ can be easily measured using the cutback

method [8]; details of the measurement procedure are given in section 3.4.

As a result of the above discussion, it can be seen that the mean overlap integral can be calculated from its equivalent expression shown in equation (2.14), which contains the parameters τ, $\omega(\lambda)$, and $g_s(\lambda)$, that can be determined both simply and accurately.

In commonly used erbium-doped fibers, erbium is confined to 20% - 50% of the fiber core area [46]. For such fibers, it can be shown that the mode power distribution, $\psi_s(\lambda, r)$, over the entire emission spectrum (typically $1400 \leq \lambda \leq 1650$ for silica-based erbium-doped fibers) varies by only a few percent. As an example, let us take a typical erbium-doped fiber with a core diameter of 4 μm, a numerical aperture of 0.2, and a step like erbium distribution with 50% confinement, then the absolute value of the maximum difference among the overlap integrals in the 1400-1650 *nm* wavelength range is only 2.36%. These discrepancies for cases in which the erbium-doped fiber has the same core radius and numerical aperture, but confinements of 40%, 30%, and 20%, were calculated to be 1.51%, 0.85%, and 0.37%, respectively. Consequently, using the mean overlap integral as the value of the overlap integral for the entire emission spectrum, introduces only a few percent error. In addition, since in the mean overlap integral, λ^* is a wavelength between the limits λ_1 and λ_2, intuitively near the middle of the emission spectrum, the errors caused by replacing it as the value of the overlap integral for the entire emission spectrum would be even less than the maximum discrepancy evaluated before. For the fiber in the above example with 50% erbium confinement, by assuming $\lambda^* = 1525\,nm$, the absolute value of the maximum difference between the mean overlap integral at λ^*, and the ones in the wavelength range 1400-1650 *nm* is only 1.22%. This shows that the mean overlap integral, which can be simply calculated using equation (2.14), can be

actually substituted for the overlap integrals over the entire emission spectrum of the ${}^4I_{13/2} \rightarrow {}^4I_{15/2}$ transition in erbium-doped fibers. Once the mean overlap integral is calculated, one can simply calculate the emission cross-sections using equation (2.2). The absorption cross-sections can then be simply calculated either using equation (C.3), or equation (2.4). Figure 2.4 shows calculated emission and absorption cross-sections for a germano-alumino silicate erbium-doped fiber (fiber #5) having a cutoff wavelength of 850 *nm,* a core radius of 1.8 μm, a numerical aperture of 0.18, and a fluorescence lifetime of $\tau = 10.15$ *ms*. The measured spectral absorption coefficient and the normalized fluorescence of this fiber are shown in Figures 2.5 and 2.6, respectively. Also, Figure 2.7 shows a comparison between the measured fluorescence and the one calculated from the absorption coefficient data using equation (2.12).

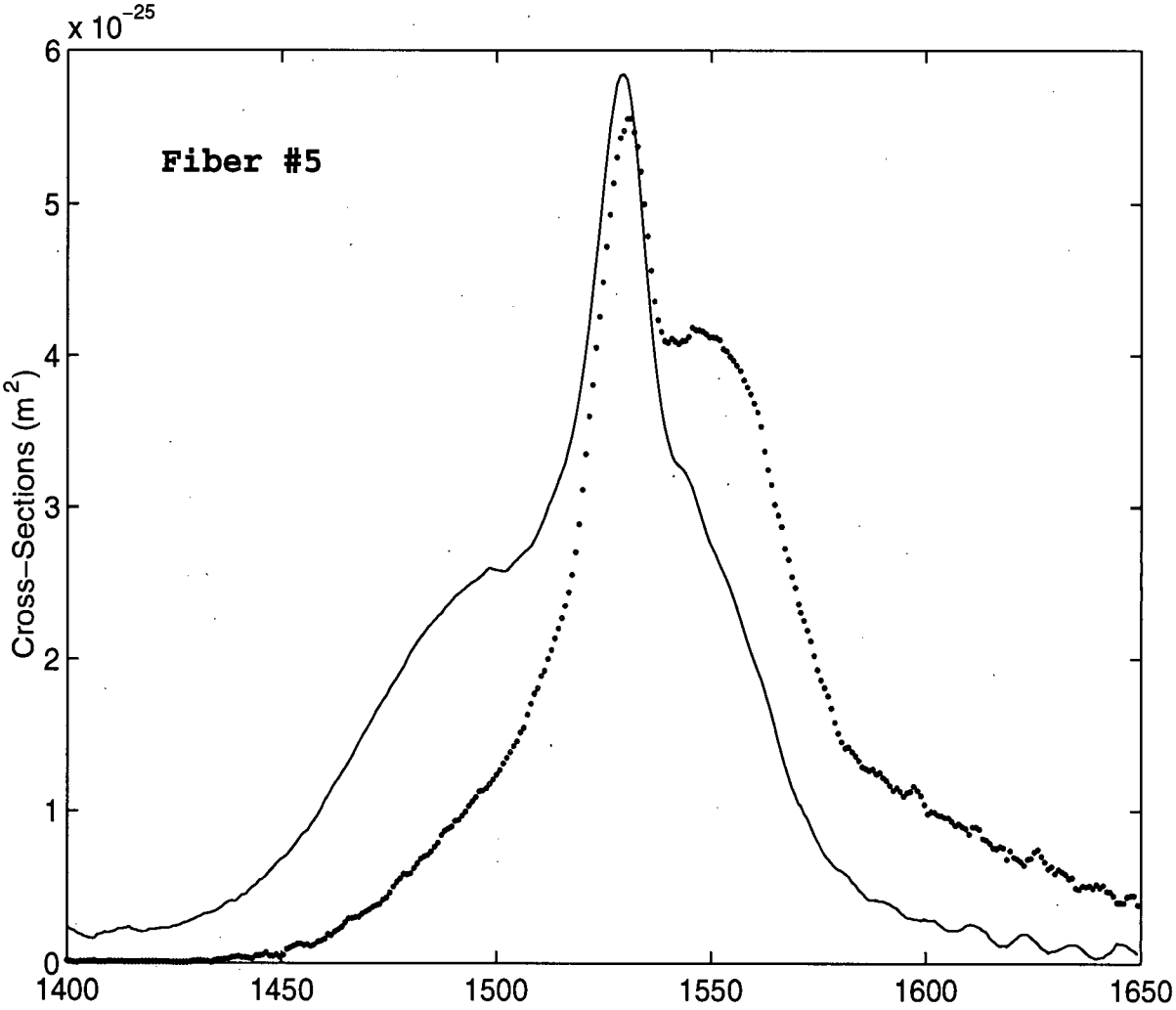

Figure 2.4. Calculated absorption cross-sections (solid) and emission cross-sections (dotted) for fiber #5.

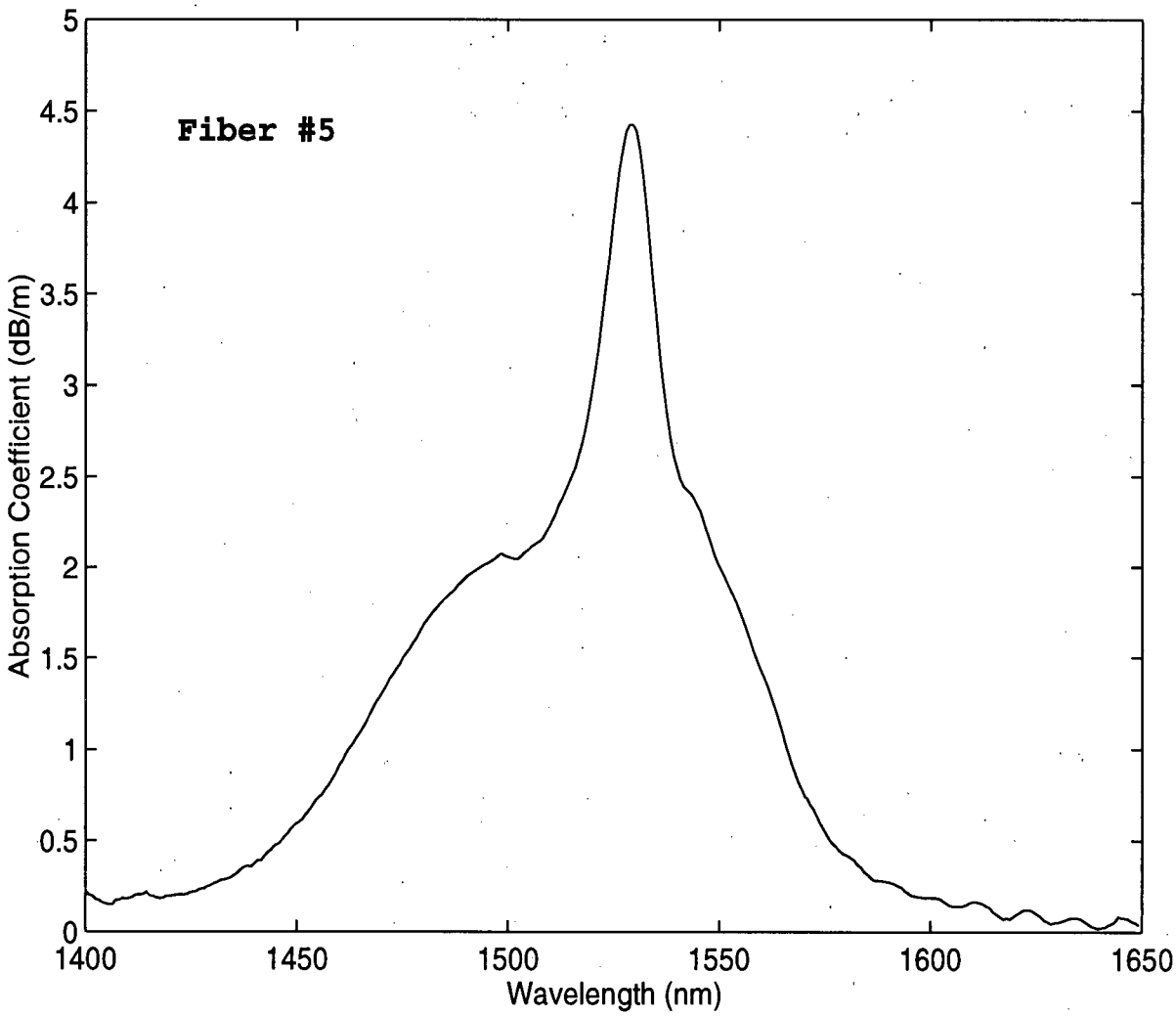

Figure 2.5. Measured absorption coefficient of fiber #5.

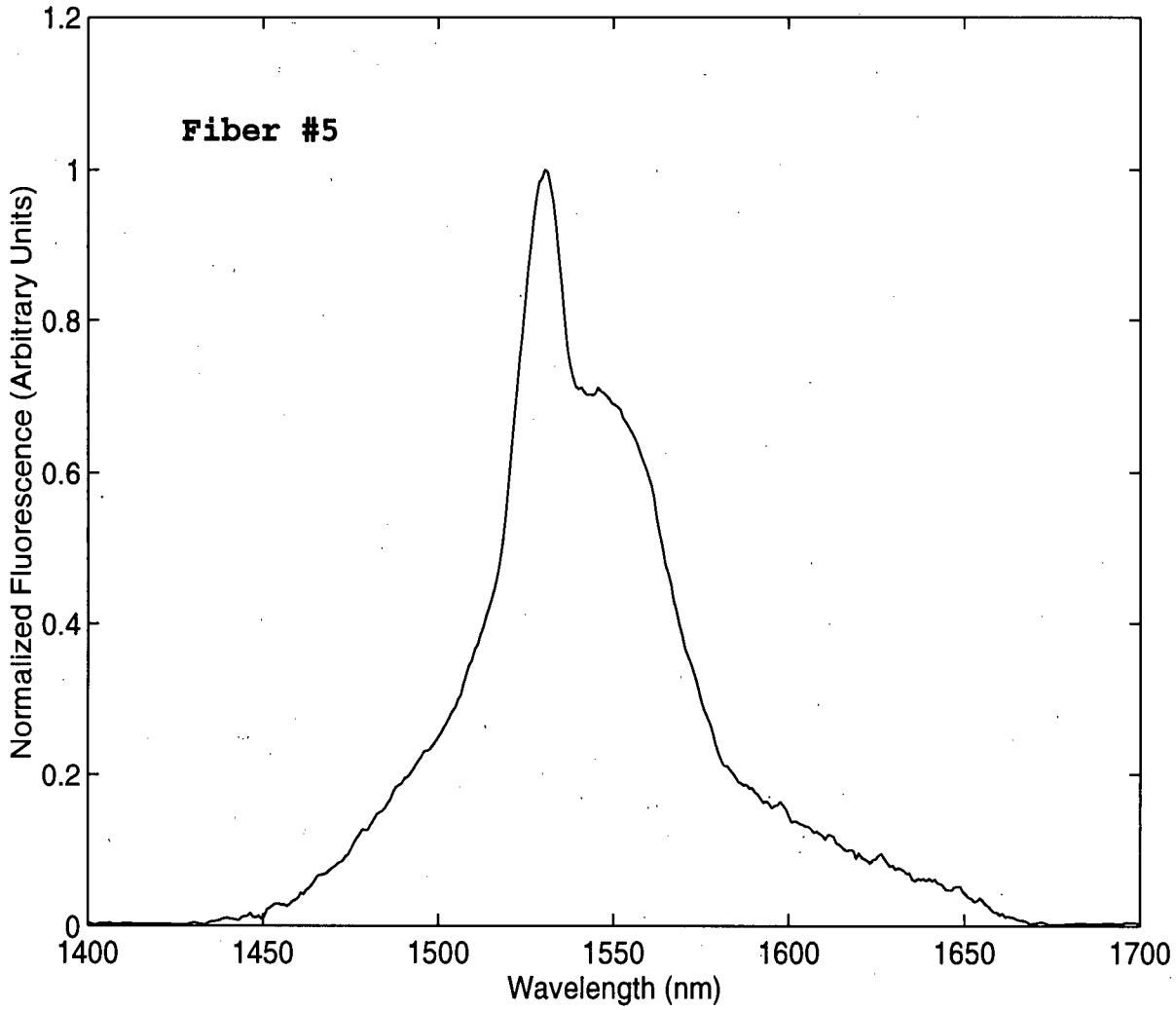

Figure 2.6. Measured fluorescence of fiber #5. The fluorescence spectrum is normalized with respect to its peak value.

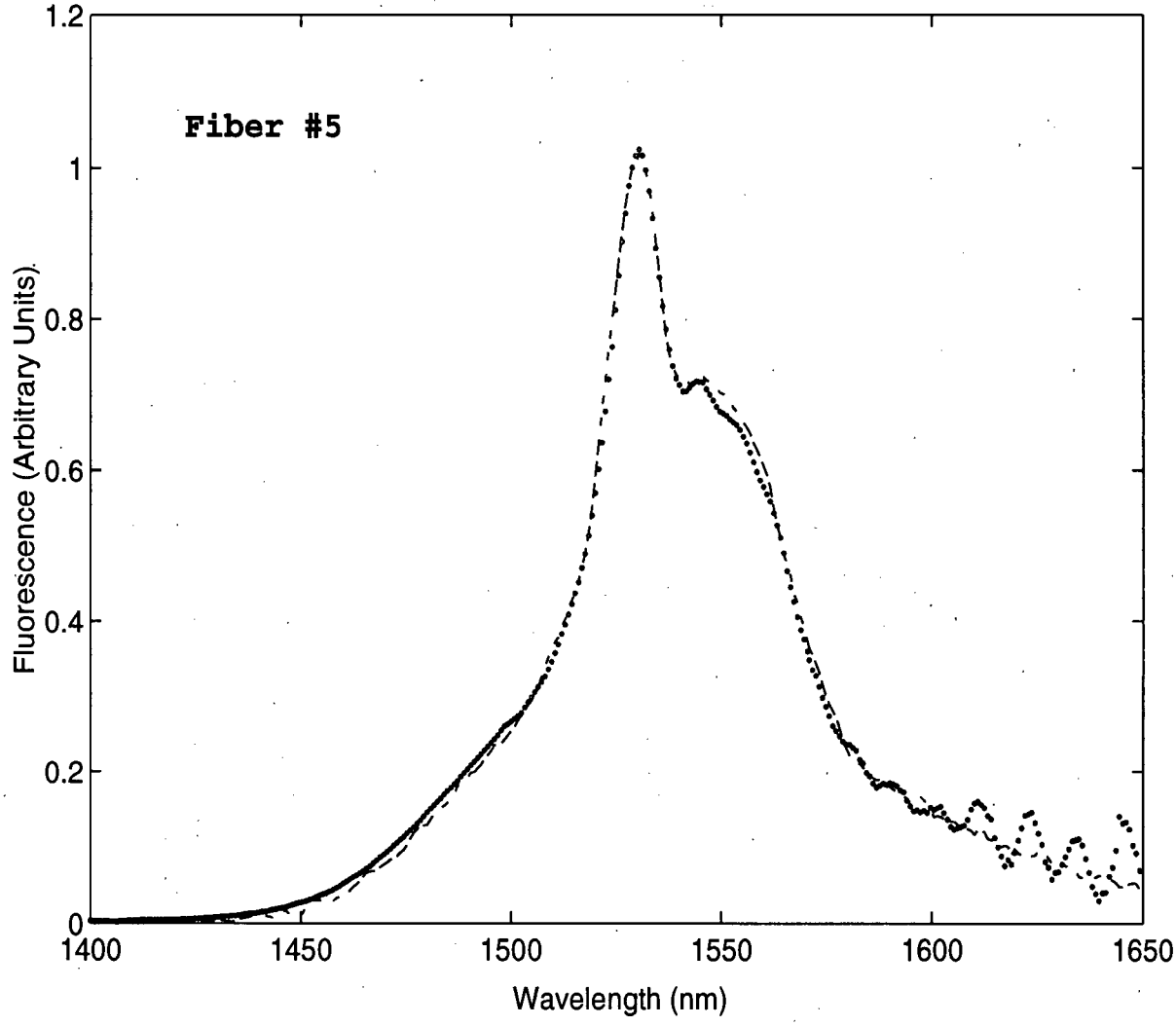

Figure 2.7. Comparison between the measured fluorescence (dashed) and calculated fluorescence (dotted). Both spectra are normalized with respect to their values at λ_{peak}.

The saturation power at signal wavelengths, $P_{sat}(\lambda)$, defined in equation (B.17), is a function of the absorption and emission cross-sections, mode power radius, and fluorescence lifetime. But, due to the uncertainty which exists regarding the actual values of cross-sections, this parameter is commonly calculated by a technique first proposed by Saleh *et. al.* [49]. According to this technique, $P_{sat}(\lambda)$ can be determined based on measured monochromatic absorption data using:

$$P_{out}(\lambda) = P_{in}(\lambda)\, e^{-\alpha_s(\lambda)L}\; e^{(P_{in}(\lambda) - P_{out}(\lambda))/P_{sat}(\lambda)}\,, \tag{2.21}$$

where $P_{in}(\lambda)$ is the power of a monochromatic beam at wavelength λ into a piece of erbium-doped fiber, $P_{out}(\lambda)$ is the power of the beam at the output of the fiber, and L is the length of the fiber. To check the accuracy of the cross-sections calculated using our method, we calculated $P_{sat}(\lambda)$ at $\lambda = 1530\ nm$ and $\lambda = 1550\ nm$ using equation (B.17), and compared those with the measured $P_{sat}(\lambda)$ using the above technique proposed by Saleh *et. al.* (Details of the measurement procedure for obtaining $P_{sat}(\lambda)$ are given in section 3.6). Table 2.2 gives the calculated and measured values of $P_{sat}(\lambda)$ at the two wavelengths, together with the absolute value of the maximum discrepancy between them.

Table 2.2. Measured and calculated values of $P_{sat}(\lambda)$ at wavelengths $\lambda = 1530\ nm$ and $\lambda = 1550\ nm$.

Wavelength (nm)	Measured P_{sat} (mW)	Calculated P_{sat} (mW)	Discrepancy Between Measured and Calculated P_{sat}
1530	0.1767	0.1826	3.3%
1550	0.2921	0.3099	6.1%

The close agreement between the measured and the calculated $P_{sat}(\lambda)$ confirms the accuracy of the calculated cross-sections using our method.

2.5. Evaluation of the erbium concentration inside the fiber core

The erbium density distribution, $\rho(r)$, in the core of the erbium-doped fibers is one of the parameters that greatly affects the performance of an optical amplifier. Theoretical studies, [16], [46], [50], have shown that a change in erbium density distribution would result in a change in gain, gain coefficient, and optimal length of an optical amplifier. Therefore, knowledge of this parameter is of great importance for accurate modeling of fiber amplifiers and is also important for improving the techniques used to design and manufacture erbium-doped fibers.

A direct measurement of the erbium concentration profile in the fiber core is a challenging task. This is due to the small size of the fiber core (typically having a diameter of about 4 μm). Previous attempts to determine this parameter, such as secondary ion mass spectrometry (SIMS) and electron probe microanalysis (EPMA) in conjunction with X-ray fluorescence (XRF), have been based on measurements performed on slices of partially drawn, thick preforms [28], [51]. The accuracy of these measurements is estimated to be about 18% [28] and, as was explained in section 2.3, the final draw of the preform into the actual fiber will cause redistribution of the erbium ions, resulting in additional errors. Recently D. Uttamchandani *et. al.* [21] have proposed a technique which allows direct determination of the erbium profile in the fiber core. In this technique short lengths of erbium-doped fibers (approximately 1 *mm* long) are pumped by a laser beam, and the generated fluorescence at the output of the fiber, across the fiber core, is imaged using a confocal optical microscope. Since the intensity of the generated fluorescence is proportional to the erbium concentration, the erbium distribution inside the fiber core can be determined. Although this technique allows the shape of the erbium distribution to be determined, it cannot provide the actual concentration.

Here, we show that, once the erbium distribution is known, the erbium concentration inside the fiber core can be calculated using our closed-form expression, equation (2.13). We define, ρ_0 to be the peak value of $\rho(r)$. Accordingly, equation (2.13) can be written as:

$$\rho_0 = 4\pi c n^2 \tau \int_{\lambda_1}^{\lambda_2} \frac{\omega_s^2(\lambda)\, g_s(\lambda)}{\lambda^4 \int_0^{\infty} \frac{\rho(r)}{\rho_0} \psi_s(\lambda, r) r dr} d\lambda \ , \qquad (2.22)$$

where $\rho(r)/\rho_0$, is the normalized erbium distribution, i.e., the shape of the erbium profile inside the fiber core. Since all of the parameters on the right hand side of equation (2.22) can be either measured or evaluated, by using this equation ρ_0 can be determined.

Summary of Chapter 2

In this chapter the theory of operation of single-mode erbium-doped fiber amplifiers pumped at 980 *nm* has been described. Based on the general rate equation, and McCumber's theory of phonon-terminated optical masers, two closed form expressions have been derived. In one of them, the fluorescence spectrum of an erbium-doped fiber is related to its spectral absorption coefficient. Based on this expression, a rigorous basis for the assessment of the applicability of McCumber's theory to the study of ${}^4I_{13/2} \Leftrightarrow {}^4I_{15/2}$ transitions in erbium-doped fibers has been established. For the cases of five silica-based erbium-doped fibers, experiments were performed and the results were used to validate this expression. The other closed form expression, provides a simple means for calculating absorption and emission

cross-sections of erbium-doped fibers using the easily measured spectral absorption coefficient, the gain coefficient at one particular wavelength, and the fluorescence lifetime. Also, based on this expression, an analytical method for the simple determination of the erbium ion concentration inside the fiber core has been proposed.

Experiments were performed to evaluate the spectral cross-sections of an erbium-doped fiber over the wavelength range 1400-1650 *nm*, and the accuracy of the calculated cross-sections was ensured by comparing the measured values of saturation powers at 1530 *nm* and 1550 *nm* with the ones calculated using the values of the cross-sections.

Chapter 3

Experimental Techniques and Measured Results

3.1. Introduction

In order to evaluate the absorption and emission cross-sections of an erbium-doped fiber at signal wavelengths, using the technique described in chapter 2, several fiber parameters such as the spectral absorption coefficient, $\alpha_s(\lambda)$, spectral fluorescence, $F(\lambda)$, gain coefficient, $g_s(\lambda)$, and fluorescence lifetime, τ, have to be measured.

In the evaluation of these parameters, while $\alpha_s(\lambda)$ and $g_s(\lambda)$ were determined using the conventional cutback technique, for the measurement of spectral fluorescence, a new setup was designed to measure the fluorescence in the backward direction, as opposed to the forward direction which is the direction of pump light propagation. This technique provides a simpler, and more accurate means for the measurement of spectral fluorescence as compared with the conventional techniques by which the fluorescence is measured either in the forward direction or from the side of the fiber [7], [43], [44], [52]. Also, in determining the fluorescence lifetime, τ, unlike conventional techniques in which τ is determined from the fluorescence intensity measured in the forward direction [15], [44], [53] or from the side of the fiber [7], [54], we determined τ using the fluorescence intensity measured in the backward direction. In this way we have managed to simplify the experimental procedure for determining this parameter.

In order to examine the accuracy of the calculated cross-sections using our technique, as was described in section 2.4, the saturation power at signal wavelengths was determined by performing monochromatic absorption measurements.

3.2. Measurement of the spectral absorption coefficient

The spectral absorption coefficient of erbium-doped fibers is an essential parameter used in numerical models for EDFAs [15]. It is also used to determine the location and the strength of the possible pump bands [43]. This parameter was measured by the standard cutback method [55].

A schematic of the experimental setup is illustrated in figure 3.1. The light source is a MRV Communications MREDSP5000 broad-band LED, 1400-1700 *nm,* with an output power of 5 μW, and having a single-mode fiber pigtail.

In order to couple the light of the LED into the erbium-doped fiber a fusion splice was used. To prepare the fibers for fusion splicing, the end of the LED's fiber and one end of an erbium-doped fiber, were soaked in trichloroethylene for about one minute to loosen their jackets. Afterwards about 6 centimeters of the jackets were removed from each of the fiber ends, the ends were cleaved using York FK11 fiber cleaver and, finally, the cleaved ends of the fibers were fusion spliced together using a Northern Telecom NT7L30AB video fusion splicer. To strip out any light that may have been launched into the cladding of the erbium-

doped fiber, the regions of the doped fiber adjacent to the splice were covered with index-matching fluid index-matching fluid.

To monitor the spectral output power, the other end of the erbium-doped fiber was connected to an Anritso MVO2 optical spectrum analyzer (OSA), using an Anritso MA915A fiber adaptor and, to record the data, the OSA was connected via its GP-IB to an IBM PC compatible computer.

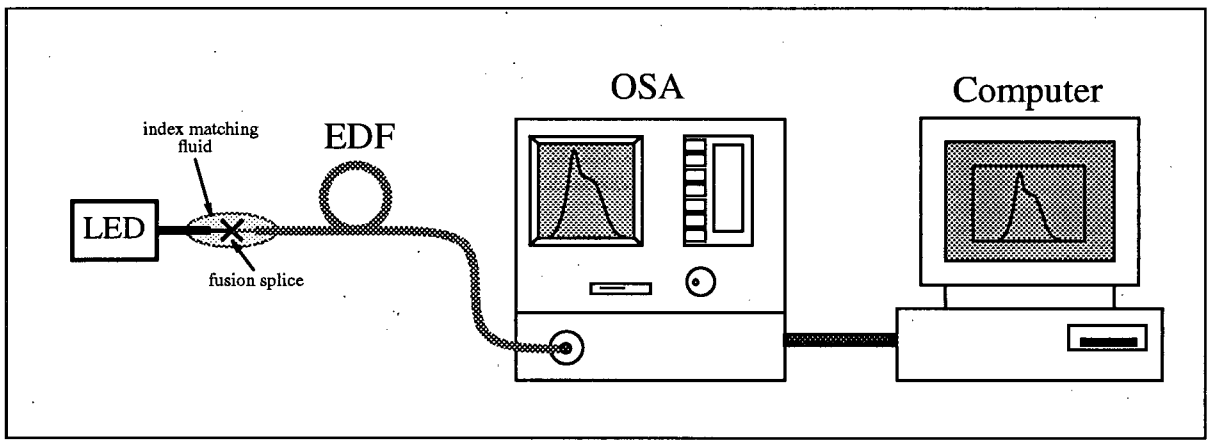

Figure 3.1. Schematic of the experimental setup used for the measurement of the spectral absorption.

To determine the fiber's absorption coefficient, the transmitted optical power $P_A(\lambda)$, as a function of the optical wavelength, was measured for a given fiber length. The fiber was then cutback, by cutting away a length, L, of the fiber at its output end, and the corresponding transmitted optical power spectra $P_B(\lambda)$ was measured again. The absorption coefficient, $\alpha_s(\lambda)$ (in decibels per meter), was then calculated from the relation [7], [52]:

$$\alpha_s(\lambda) = 10 \frac{\log\left(\frac{P_B(\lambda)}{P_A(\lambda)}\right)}{L} . \qquad (3.1)$$

To ensure the reproducibility and consistency of the results for each fiber, several cutbacks were performed. Typical absorption coefficient spectra are shown in figures 2.3 (a)-(d) and 2.5.

Finally, in order to verify the validity of the assumption, that $P_s(\lambda, z) \ll P_{sat}(\lambda)$, made in the derivation of equation (2.4), the remaining length of the doped fiber was cut and the spectral power, which in this case was the signal power at the input of the erbium-doped fiber (EDF), i.e., $P_s(\lambda, z=0)$, was measured. For the resolution of the OSA set to 1 *nm,* the maximum value of the spectral input power was $-39\,dBm = 0.126\,\mu W$, at the wavelength $\lambda = 1556\,nm$. Since the measured $P_{sat}(\lambda = 1550\,nm)$ is $0.2921\,mW$, see Table 2.2, the above assumption is valid.

3.3. Measurement of the fluorescence spectrum

The fluorescence spectra provide information on the possibility of obtaining gain over a particular wavelength range of interest [7]. Furthermore, from the fluorescence spectrum and by measuring the gain coefficient at only one particular wavelength, the spectral gain coefficient, an essential parameter in numerical models for EDFAs [15], can be easily evaluated

using our closed form expression derived in section 2.3, equation (2.20).

Traditionally the fluorescence spectrum has been measured either in the forward direction, the direction of the pump light propagation, or from the side of the fiber [7], [43], [44], [52], [54]. In the forward detection technique [7], [43], [44], the fluorescence is measured at the output of a very short length of erbium-doped fiber (typically a length sufficiently short so that the peak of the small signal absorption is less than 0.2 *dB*), pumped with a laser operating at 980 *nm* having a typical output power of 100 *mW*. The length of the fiber is chosen to be short, in order to keep the total fiber gain small, thus avoiding distortion of the fluorescence profile due to the stimulated emission. Furthermore, high pumping powers allow full medium inversion to be achieved along the entire fiber length, avoiding distortion of the fluorescence profile due to the absorption corresponding to the ${}^4I_{15/2} \rightarrow {}^4I_{13/2}$ transitions of the erbium ions. However, since the fluorescence and the pump light are propagating in the same direction, when detecting the fluorescence the laser noise in the spectral range of the fluorescence profile is also being detected; as the power of the fluorescence is very weak, the laser noise may distort its profile. In the side detection technique [7], [52], [54], the fluorescence is, instead, being detected from the side of an erbium-doped fiber, using a very sensitive detector. In this technique, since the optical spectrum analyzer cannot be used to record the fluorescence spectrum, a somewhat complicated setup which includes a transimpedance amplifier, a lock-in amplifier, a monochromator, and data processing equipment are used [7]. In addition, since the measured spectrum is normally distorted by the wavelength dependence of the detector and by the efficiency of the monochromator, subsequent corrections have to be made [7], making the procedure even more complicated.

To avoid the problems associated with the above-mentioned techniques, a new setup was designed to measure the fluorescence in the backward direction. Figure 3.2 shows a schematic of the experimental setup used. In this experiment, the pump source was a Seastar Optics LD-2000 InGaAs-GaAs laser diode (LD) operating at 980 *nm* with 90 *mW* of output power, and had a connectorized single-mode fiber pigtail. The LD was connected to the 980 *nm* arm of a 2×1, single-mode, 980/1550 *nm* Gould Electronics wavelength division multiplexer (WDM). The connection between the ends of the connectorized fibers of the LD and the 980 *nm* arm of the WDM was made by using an OZ Optics PMPC-03 fiber adaptor. A short piece of doped fiber, having a peak small signal absorption less than 0.2 *dB,* was fusion spliced to the 980/1550 *nm* arm of the WDM, its exit end was broken and immersed in an index-matching fluid to avoid reflections. The backward fluorescence, $F^*(\lambda)$, was then collected at the WDM's 1550 *nm* arm using the optical spectrum analyzer and was recorded using an IBM PC compatible computer attached to the OSA. By using this technique, we managed to eliminate the laser noise in the measurement of the fluorescence spectrum, as the laser light was propagating in the forward direction.

Since the WDM normally has a non-uniform spectral response, accordingly the measured fluorescence had to be corrected to give the actual fluorescence spectrum, $F(\lambda)$. Therefore, the spectral response of the WDM was measured over the wavelength range 1400-1700 *nm.* To measure the WDM spectral response, the output end of the broadband LED, used in the absorption measurement, was fusion spliced to the 980/1550 *nm* arm of the WDM, and the transmitted light, $T_1(\lambda)$, was collected at the WDM's 1550 *nm* arm using the OSA and recorded using the attached computer. Separately, the spectral response of the LED, $T_2(\lambda)$,

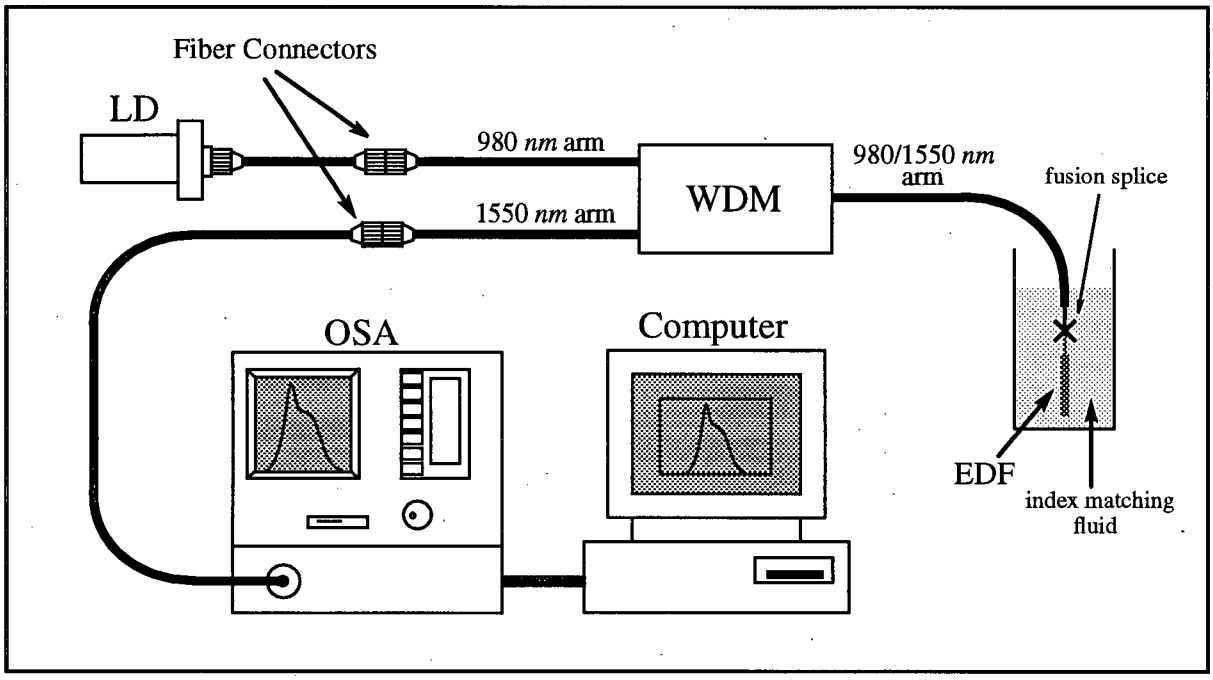

Figure 3.2. Schematic of the experimental setup used for the measurement of the fluorescence spectrum.

was measured by directly connecting the LED's fiber end to the OSA. To eliminate the effect of coupling loss due to fusion splicing in the measurement of $T_1(\lambda)$, both small-signal gain the measured spectra, i.e., $T_1(\lambda)$ and $T_2(\lambda)$, were normalized with respect to their peak values. Finally, the normalized spectral response of the WDM, T_{WDM}, was evaluated by dividing $T_1(\lambda)$ by $T_2(\lambda)$ and normalizing the result with respect to its peak value. Figure 3.3 shows the normalized spectral response of the WDM in the wavelength range 1400-1700 *nm*. By knowing T_{WDM}, the actual shape of the fiber's fluorescence spectra, $F(\lambda)$, was calculated from the measured fluorescence spectra, $F^*(\lambda)$, using the relationship $F(\lambda) = F^*(\lambda) / T_{WDM}(\lambda)$. The normalized fluorescence spectrum was then obtained, by normalizing $F(\lambda)$ with respect to its peak value. Figure 2.6 shows a typical normalized fluorescence spectrum

measured in the wavelength range 1400-1700 *nm*.

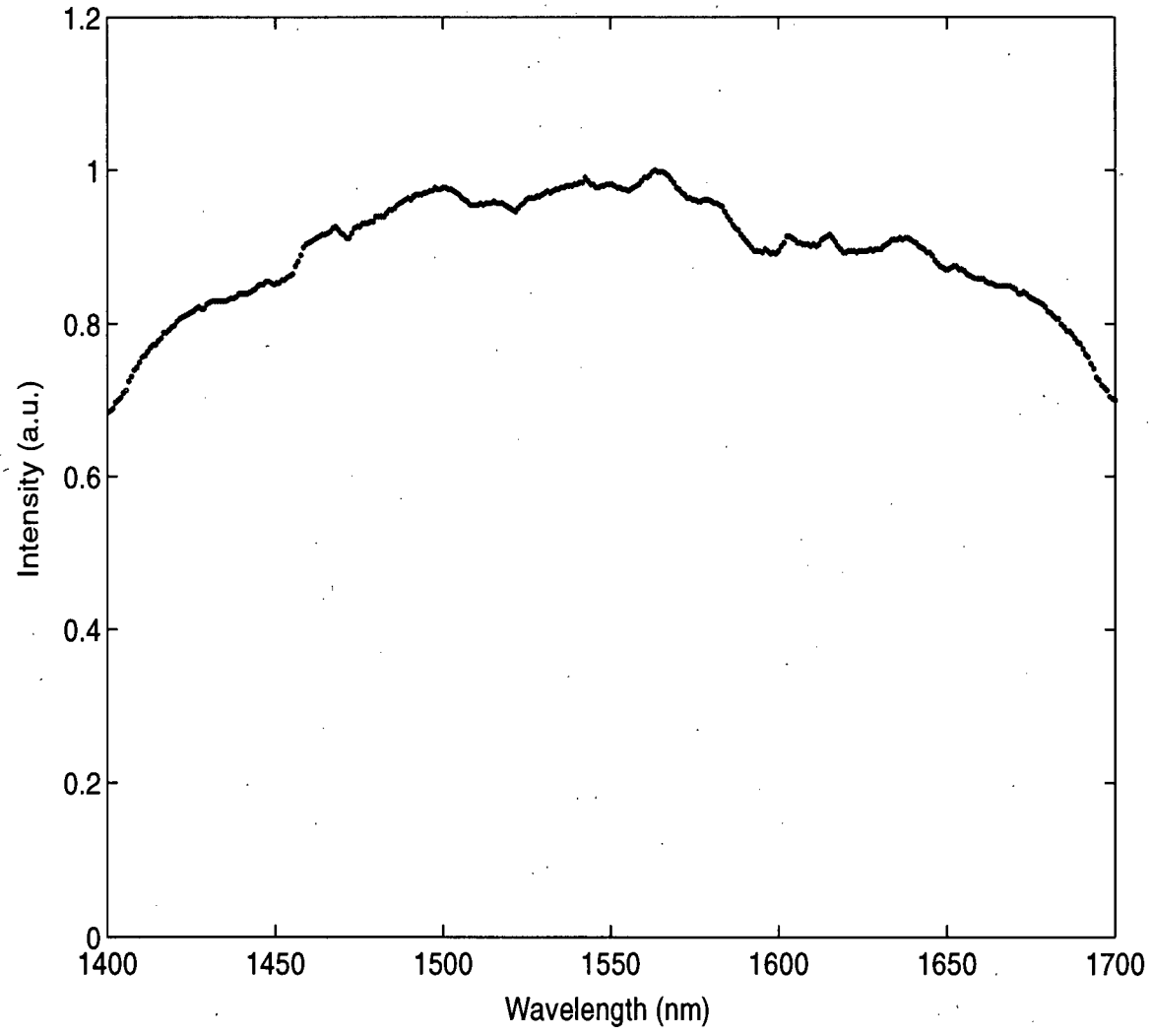

Figure 3.3. Spectral response of the WDM, normalized with respect to its peak value.

3.4. Measurement of the small-signal gain coefficient

The small-signal gain coefficient, $g_s(\lambda)$, is one the essential parameters in the numerical models for EDFAs [15]. As is the case for the absorption coefficient, this parameter is measured using the standard cutback technique [8]. Figure 3.4 shows a schematic of the experimental setup used for the measurement of the gain coefficient.

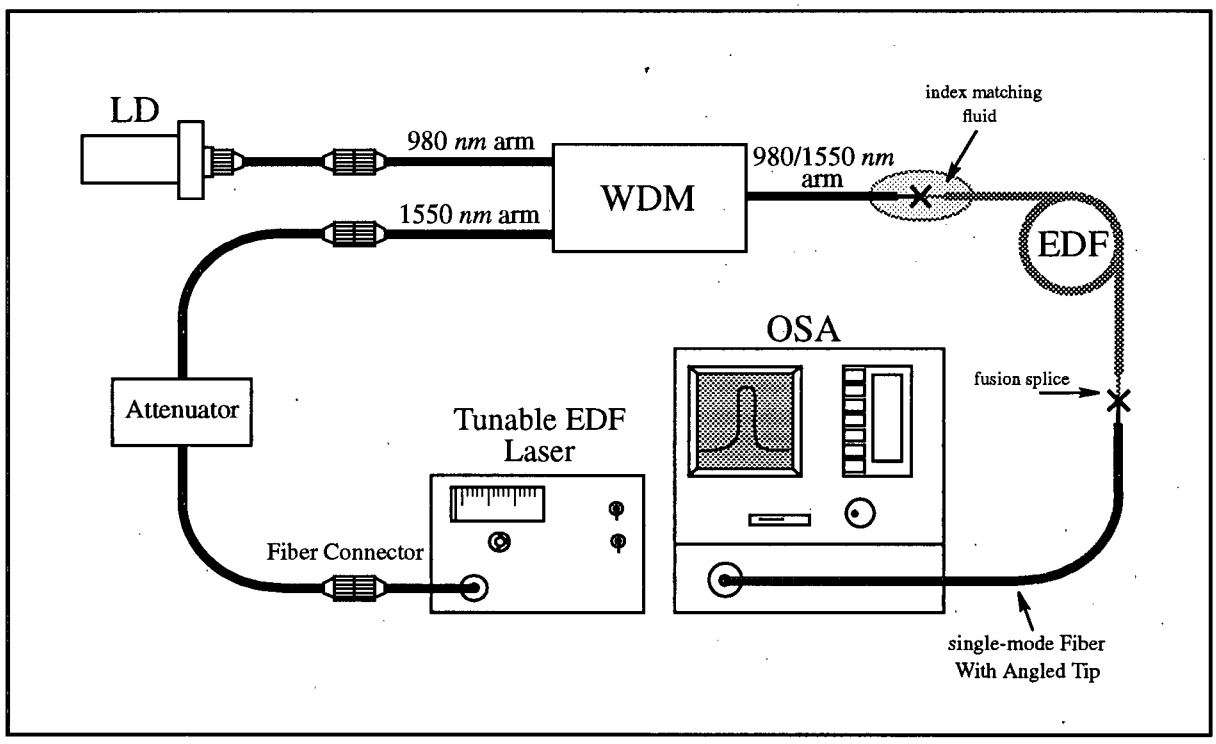

Figure 3.4. Schematic of the experimental setup used for the measurement of the gain coefficient.

To be specific, the experimental procedure for the measurement of the gain coefficient is

described using a particular erbium-doped fiber (EDF), fiber #5, as an example. This fiber had a cutoff wavelength of 850 *nm,* a core radius of 1.8 μm, and a numerical aperture of 0.18. The absorption coefficient spectrum and the fluorescence spectrum of this fiber are shown in Figures 2.5, and 2.6, respectively.

In this experiment, the signal source was an NOI tunable erbium-doped fiber laser (EDF laser) operating in the wavelength range 1520-1564 *nm*. To be able to adjust the level of the signal power, the EDF laser was connected to a JDS FITEL adjustable attenuator. The other end of the attenuator was connected to the 1550 *nm* arm of a 2×1, single-mode, 980/1550 *nm* Gould Electronics, WDM. The pump source was the same laser diode used in the fluorescence measurement, and was connected to the 980 *nm* arm of the WDM. A length of the EDF, 3.081 *m*, was fusion spliced to the end of the 980/1550 *nm* arm of the WDM and, to strip out the light that may have been launched into the cladding of the EDF, the regions of the doped fiber adjacent to the splice were covered with index-matching fluid. Also, in order to avoid reflections, the exit end of the EDF was fusion spliced to one end of a standard single-mode fiber having a connectorized, angled tip at its exit end (having an angle of 10° with respect to the fiber longitudinal axis). To monitor the output spectral power of the signal, the other end of the standard single-mode fiber was connected to the OSA.

The experiment was begun by tuning the signal source, the EDF laser, to operate at the peak of the fiber fluorescence spectrum, $\lambda = 1530\ nm$ (see Figure 2.6). As was explained in section 2.3, this minimizes the error introduced by uncertain values of fiber background loss $\alpha_b(\lambda)$ or when ignoring $\alpha_b(\lambda)$ in the calculation of gain coefficient. To satisfy the assumptions, $P_s(\lambda, z) \ll P_{sat}(\lambda)$ and $P_s(\lambda, z) \ll P_p(\lambda, z)$, made in the derivation of equation

(2.2), the signal power had to be adjusted appropriately. In order to do so, the pump laser was turned on and, while the spectral power of the signal was being monitored using the OSA, the attenuator was adjusted such that the measured output signal power at $\lambda = 1530\ nm$ was $-23.5\ dBm$. By neglecting the background loss of the standard single-mode fiber (~ 0.2 *dB/km* at $\lambda = 1550\ nm$), and the splice loss (typically 0.05 *dB*), we can write $P_s(\lambda, z{=}L{=}3.081m) = -23.5\ dBm$. This is 188 times larger than the saturation power of fiber #5, which is $0.1767mW = -0.75\ dBm$ (see Table 2.2). Since $P_s(\lambda, z{=}L)$ is the maximum value of the $P_s(\lambda, z)$, it is clear that the assumption $P_s(\lambda, z) \ll P_{sat}(\lambda)$ is valid. To measure the pump power, the end of the standard single-mode fiber was disconnected from the OSA, and connected to a Newport 840 optical power meter. The pump power was measured to be 71 *mW*=18.75 *dBm*. Since this is the minimum value of $P_p(\lambda_p, z)$, and $P_s(\lambda, z{=}L)$ is the maximum value of $P_s(\lambda, z)$, the assumption $P_s(\lambda, z) \ll P_p(\lambda, z)$ is clearly valid. The end of the standard single-mode fiber was reconnected to the OSA, and the spectral power of the output signal was monitored using the OSA. In Figure 3.5 this spectrum is shown by a plot designated as "output". From this spectrum, the signal power level was measured $P_A^*(\lambda) = -23.5\ dBm$. The spectrum also shows the level of the noise power around the signal wavelength. The level of the noise power at the signal wavelength cannot be measured directly because the signal power level masks the noise level at this wavelength; instead it can be determined using the interpolation technique [56]. In this technique, the noise level at the signal wavelength is determined by measuring the noise level at wavelengths just above and just below the signal wavelength and then, by interpolation, the noise level at the signal wavelength is determined. Using this technique, the noise power level of the spectral output power,

designated as "output" in Figure 3.5, was measured to be $N_{out} = -44.25\ dBm$. This amount of noise, which is the total output noise power within the optical spectrum analyzer's resolution bandwidth at the signal wavelength, is related to the ASE power of the EDFA, P_{ASE}, through [56],

$$N_{out} = Gain \times N_{in} + P_{ASE} \ , \tag{3.2}$$

where N_{in} is the noise power level at the input of the EDF. To obtain the actual signal power level, $P_A(\lambda)$, N_{out} has to be subtracted from $P_A^*(\lambda)$, which gives $P_A(\lambda) = 4.43\ \mu W = -23.54\ dBm$.

To calculate the gain coefficient, the EDF was cutback, by cutting away 1.084 m of the fiber at its output end, and the corresponding spectral output power was monitored using the OSA. The signal power level at $\lambda = 1530\ nm$ was measured $P_B^*(\lambda) = -28.2\ dBm$, and the noise power level at this wavelength was measured $-48.95\ dBm$; this gives the actual signal power of $P_B(\lambda) = 1.5\ \mu W = -28.24\ dBm$. The gain coefficient, $g_s(\lambda)$ (in decibels per meter), was then calculated from the relation [7], [52]:

$$g_s(\lambda) = 10\,\frac{\log\left(\frac{P_A(\lambda)}{P_B(\lambda)}\right)}{L} \ , \tag{3.3}$$

giving $g_s(\lambda = 1530\ nm) = 4.35\ dB/m$ for fiber #5.

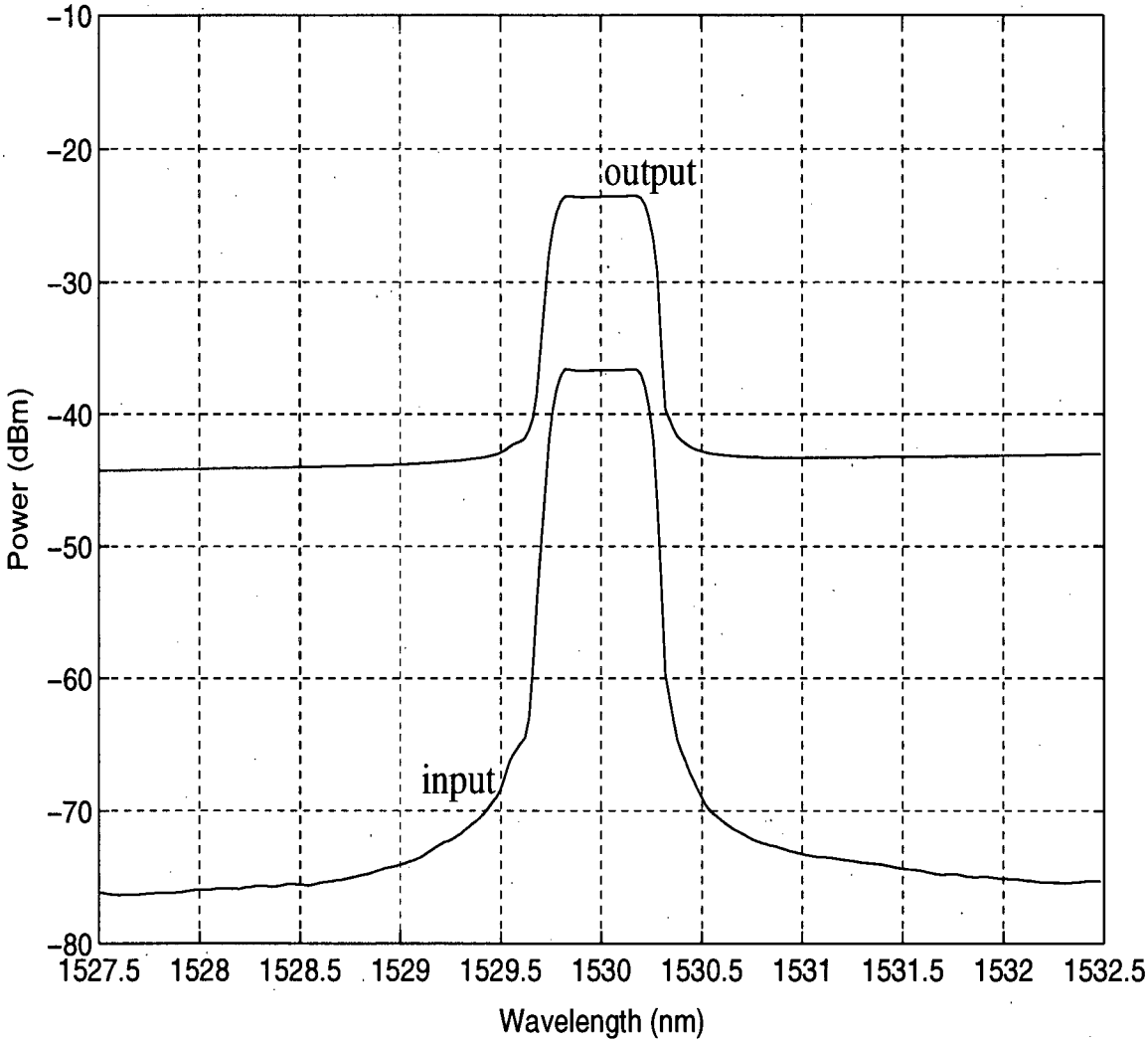

Figure 3.5. Spectral input signal power to the EDF and spectral output signal power of the EDF.

To determine the signal power and the noise power at the input of the EDF, the remaining length of the EDF was cut, and the spectral power of the input signal was monitored using the OSA. In Figure 3.5 this spectrum is shown by a plot designated as "input". From this spectrum, the signal power level at 1530 *nm* was measured, $P_C^*(\lambda) = -36.63$ *dBm*, and the level

of the noise, using the extrapolation technique, was measured $N_{in} = -76.37\,dBm$. Therefore, the actual input power is equal to $P_C(\lambda = 1530\ nm) = 0.22\mu W = -36.63\,dBm$. From the above results, the ASE power of the EDFA can be calculated, using equation (3.2), as $P_{ASE} = N_{out} - Gain \times N_{in} = 3.76 \times 10^{-8} - 18.97 \times 2.31 \times 10^{-11} = 3.72 \times 10^{-8}\,W =$ $-44.29\,dBm$; this gives a ratio of 119 between the output signal power $P_A = P_s(\lambda, z=L)$, and the total ASE power of the EDFA, $P_{ASE}(\lambda, z=L)$. From the above, and also from the fact that the signal to noise ratio improves for $z < L$, it is clear that the other assumption, $P_s(\lambda, z) \gg P_{ASE}(\lambda, z)$, made in the derivation of equation (2.2) is valid.

Finally, the last assumption, $P_p(\lambda_p, z) \gg P_{sat}(\lambda_p)$, made in the derivation of equation (2.2) also had to be validated. The value of $P_{sat}(\lambda_p = 980\ nm)$ can be estimated as follows. From the combination of equations (B.17), (B.18), (2.2), and (2.4) we can write:

$$\frac{P_{sat}(\lambda_p)}{P_{sat}(\lambda)} = \frac{\alpha_s(\lambda) + g_s(\lambda)}{\alpha(\lambda_p)} \frac{\lambda}{\lambda_p} \frac{\int_0^\infty \rho(r)\psi(\lambda_p, r) r dr}{\int_0^\infty \rho(r)\psi_s(\lambda, r) r dr}. \qquad (3.4)$$

Let us consider $\lambda = 1530\ nm$, then from the measurement of the absorption coefficient we have $\alpha_s(\lambda=1530\ nm) = 4.43\ dB/m = 1.02\ m^{-1}$ and from the measurement of the gain coefficient we have $g_s(\lambda=1530\ nm) = 4.35\ dB/m = 1.00\ m^{-1}$. Besides, $\alpha(\lambda_p)$ was measured to be $3.6\ dB/m = 0.83\ m^{-1}$ (measured by Mr. A. Croteau), using the same procedure as that described in section 3.2 except using an Anritso MG922A white light source as the signal source around 980 *nm*. The saturation power at signal wavelength, $P_{sat}(\lambda=1530\ nm)$, is

0.1767 mW (see Table 2.2). From the fact that the mode power distribution shrinks as the wavelength of the light becomes shorter, it is obvious that the ratio of the overlap integrals on the right side of equation (3.4) is less than 1. Therefore, from the above, $P_{sat}(\lambda_p = 980\ nm) < 0.67mW$. Comparing this value with the lowest level of the pump power, the pump power at the output end of the EDF, which was measured to be 71 mW=18.75 dBm, clearly validates the assumption $P_p(\lambda_p, z) \gg P_{sat}(\lambda_p)$.

3.5. Measurement of the fluorescence lifetime

The fluorescence lifetime, τ, of erbium ions in the metastable level, is another important parameter in numerical models for EDFAs [15]. This parameter can be measured by pumping a short length of erbium-doped fiber, and monitoring the decaying fluorescence intensity versus time after the pump light is chopped by a mechanical chopper. Since the fluorescence intensity decays exponentially according to $\exp(-t/\tau)$, where t denotes time, τ is simply the time interval over which the fluorescence intensity decays to $1/e$ of its peak value.

Traditionally, τ is measured using a setup illustrated in Figure 3.6 [7].

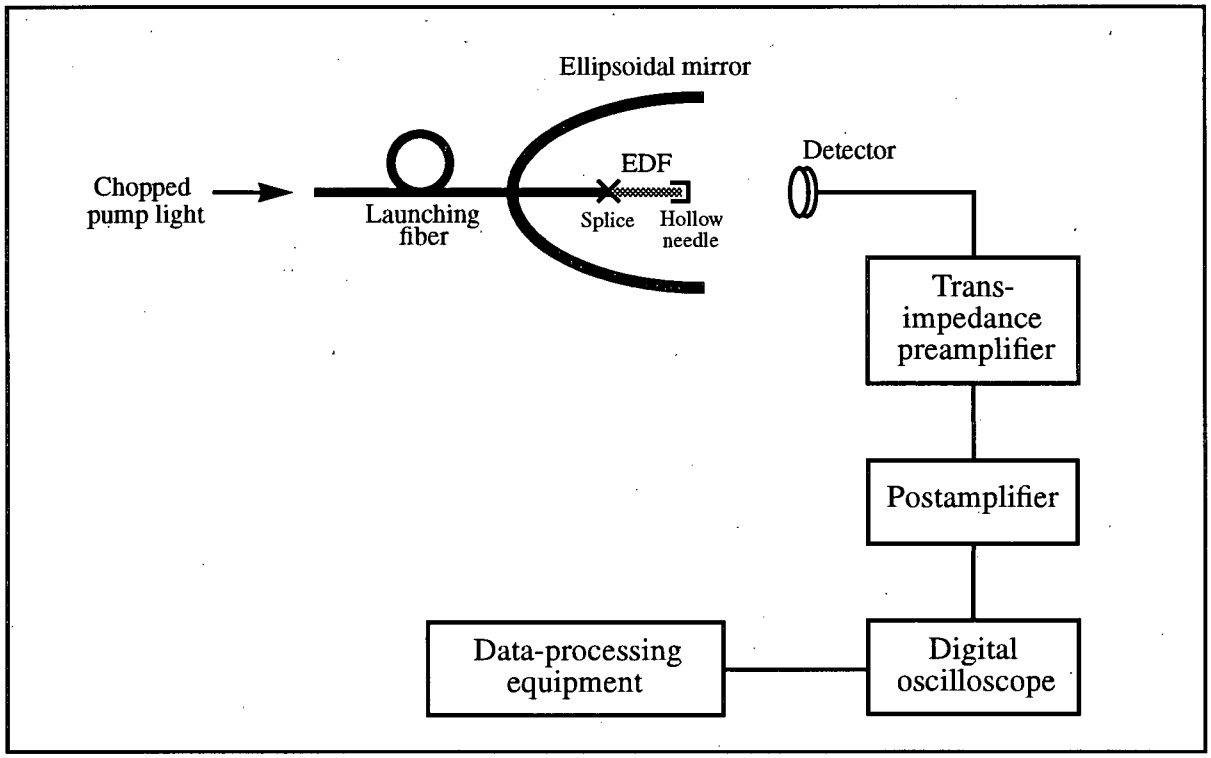

Figure 3.6. Traditional setup for the measurement of the fluorescence lifetime (form reference [7]).

In this setup, the pump light is fed through one end of a launching fiber, and a short piece of EDF is spliced to the other end. The EDF is placed in an ellipsoidal mirror in such a way that a part of the EDF coincides with one of the focal points of the mirror and, to prevent the pump light from reaching the detector, which is positioned at the other focal point of the mirror, the end of the doped fiber is placed in a hollow needle. Using this configuration, the fluorescence from sides of the doped fiber is collimated on the detector.

In order to simplify the experimental procedure, based on our new design for measuring fluorescence in the backward direction, the setup illustrated in Figure 3.7 was used to measure τ.

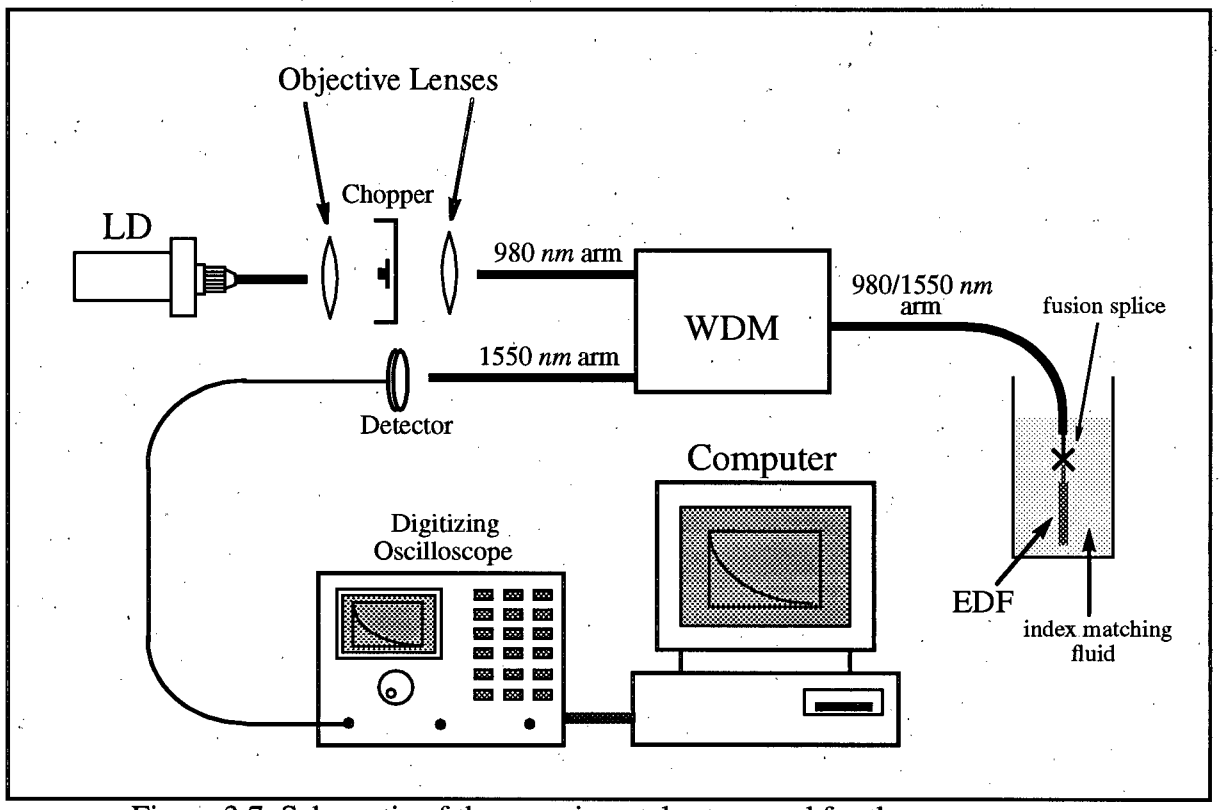

Figure 3.7. Schematic of the experimental setup used for the measurement of the fluorescence lifetime.

In this experiment, the pump light was coupled into the 980 *nm* arm of the WDM, using two 20× objective lenses positioned before and after an Alpha Omega Instruments mechanical chopper. A short piece of an erbium-doped fiber (the length was chosen such that the peak small signal absorption was less than 0.2 *dB*) was fusion spliced to the end of the 980/1550 *nm* arm of the WDM and, in order to avoid reflections, the other end of the EDF was broken and immersed in index-matching fluid. The backward fluorescence was collected from the 1550 *nm* arm of the WDM and was measured using a Germanium detector. To monitor the shape of the decaying fluorescence, the detector was connected to an HP 400Msa/s Digitizing Oscillo-

scope, and the data was recorded using an IBM personal computer connected to the oscilloscope. The value of τ was obtained, by least-squares fitting of an exponentially decaying function to the measured fluorescence decay profile; τ is simply the time constant of the fitted curve. Figure 3.8 shows the measured fluorescence decay curve and the fit used to obtain τ; for this fiber τ was calculated to be 10.15 *msec*.

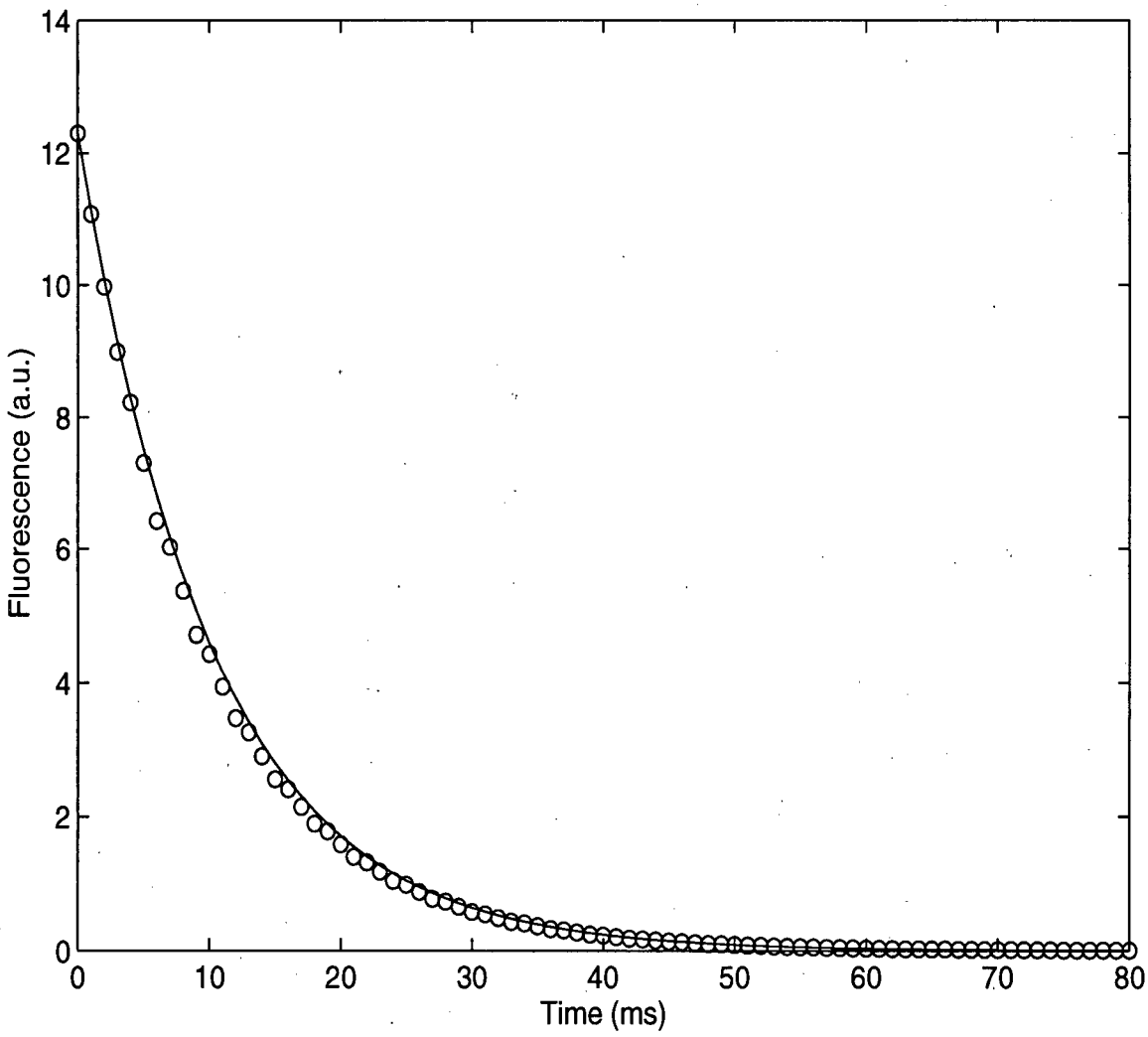

Figure 3.8. Fluorescence decay curve for the 2 *cm* long of the fiber #5 (circles). The solid line corresponds to the least-squares fit used to obtain τ.

3.6. Measurement of the saturation power at signal wavelengths

The saturation power at signal wavelengths, $P_{sat}(\lambda)$, is another important parameter in numerical models of EDFAs [49], [57]. As was discussed in section (2.4), to check the accuracy of the absorption and emission cross-sections calculated using our proposed technique, $P_{sat}(\lambda)$ was determined experimentally at $\lambda = 1530\ nm$ and $\lambda = 1550\ nm$, and the results were compared with the values of $P_{sat}(\lambda)$ calculated from equation (B.17), see Table 2.2. The experimental values of $P_{sat}(\lambda)$ were determined based on a technique proposed by Saleh *et. al.* [49]. In this technique, $P_{sat}(\lambda)$ is determined by performing a simple monochromatic absorption measurement; the absorption data is then used for the evaluation of $P_{sat}(\lambda)$ using:

$$P_{out}(\lambda) = P_{in}(\lambda)\, e^{-\alpha_s(\lambda)L}\ e^{(P_{in}(\lambda) - P_{out}(\lambda))/P_{sat}(\lambda)} \tag{3.5}$$

where $P_{in}(\lambda)$ is the power of a monochromatic beam at wavelength λ at the input of a piece of erbium-doped fiber, $P_{out}(\lambda)$ is the power of the beam at the output of the fiber, and L is the length of the fiber. The experimental setup for the measurement of $P_{sat}(\lambda)$ is illustrated in Figure 3.9.

In this experiment the monochromatic beam at the wavelength λ (in this case, λ=1530 *nm* and 1550 *nm*) was provided by using the same tunable EDF laser used in the measurement of the gain coefficient. To be able to adjust the power level of the signal, the EDF laser was connected to one end of a JDS FITEL adjustable attenuator, and the other end of the attenuator was connected to the input arm of a 1×2 single-mode 3 *dB* fused coupler (from Gould Elec-

tronics). To monitor the signal power level, one of the output arms of the coupler was connected to a Newport 840 optical power meter; the other output arm of the coupler was fusion spliced to a length of erbium-doped fiber. To strip out any light that may have been launched into the cladding of the erbium-doped fiber, the regions of the doped fiber adjacent to the splice were covered with index-matching fluid. The signal power at the output end of the EDF, $P_{out}(\lambda)$, was then measured using a Newport 818-IR S/N 746 detector attached to a Newport 835 optical power meter.

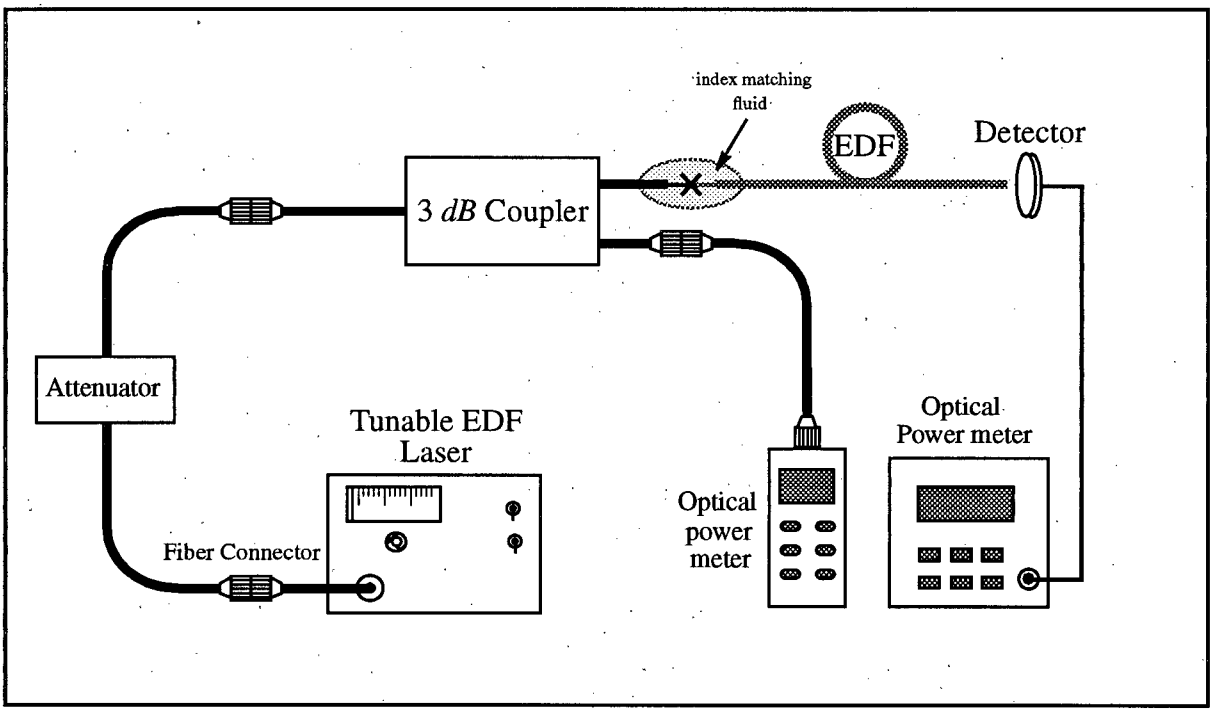

Figure 3.9. Schematic of the experimental setup used for determining the saturation power.

$P_{out}(\lambda)$ was measured over a range of input signal power levels, by a sequential adjustment of the attenuator. To keep track of these adjustments, the reading on the monitoring opti-

cal power meter was recorded each time. Finally, the EDF was cut and $P_{in}(\lambda)$ was measured over the same range of input signal power levels as it was in the measurement of $P_{out}(\lambda)$ (this was done by a sequential adjustment of the attenuator such that the readings in the monitoring optical power meter remained the same as the ones recorded for the measurement of $P_{out}(\lambda)$). Figures 3.10 and 3.11 show the experimental transmission characteristics, $P_{out}(\lambda)/P_{in}(\lambda)$, of 3.781 *m* of the fiber #5 at wavelengths of 1530 *nm* and 1550 *nm* as functions of input power, $P_{in}(\lambda)$, respectively. Knowing the value of $\alpha_s(\lambda)$ from the absorption coefficient measurement, $P_{sat}(\lambda)$ was obtained by solving the equation (3.5) in a least squares sense [73]. For fiber #5, the values of $P_{sat}(\lambda)$, determined according to the above approach, at wavelengths 1530 *nm* and 1550 *nm* are listed in Table 2.2 under the measured $P_{sat}(\lambda)$. After obtaining $P_{sat}(\lambda)$, $P_{out}(\lambda)$ was calculated from equation (3.5) and using the values of $\alpha_s(\lambda)$, $P_{in}(\lambda)$, and *L*, at both wavelengths. The solid lines in Figures 3.10 and 3.11 correspond to the analytical solutions of equation (3.5), which, in fact, represent the least square fits to the experimental transmission characteristics.

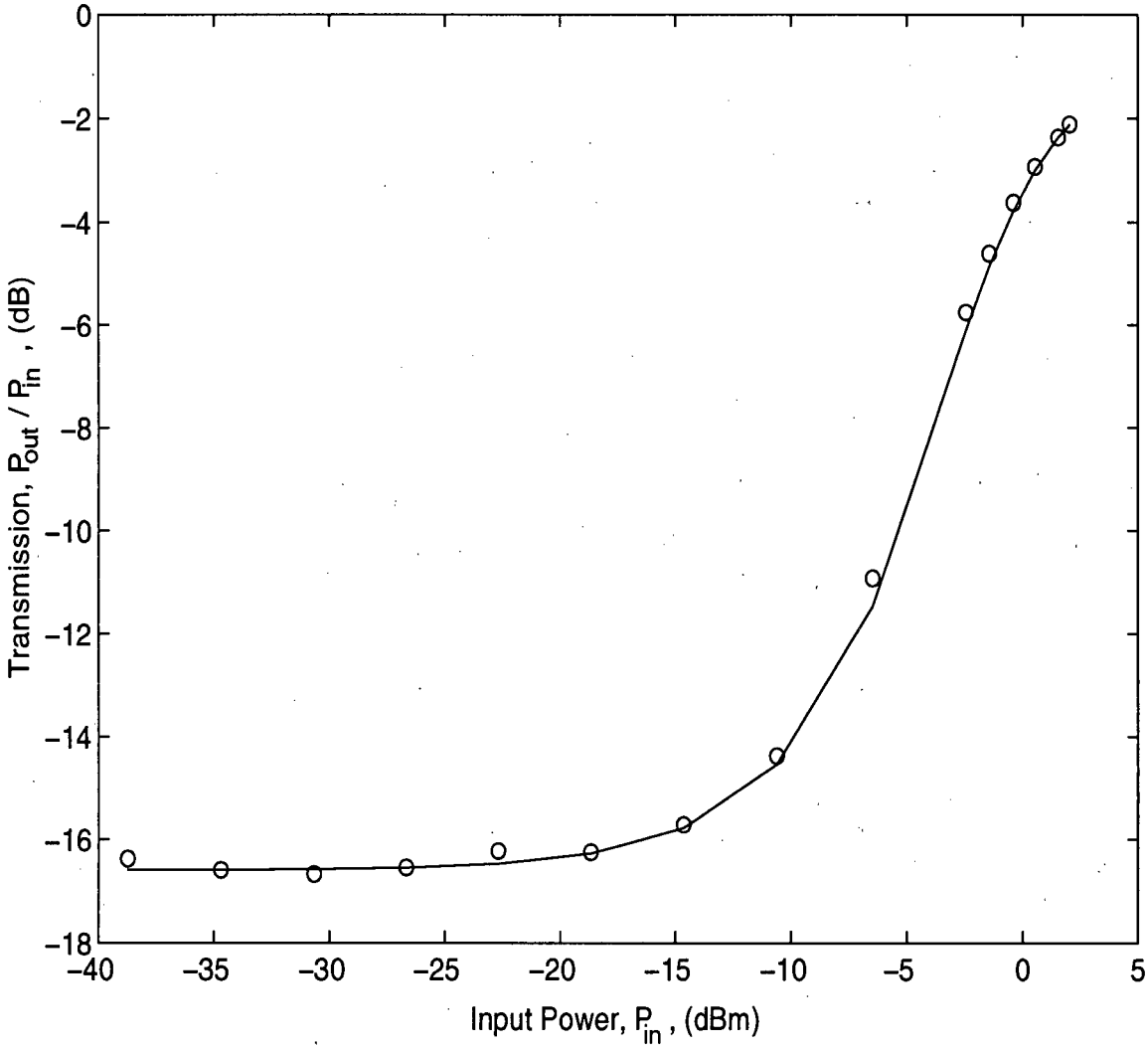

Figure 3.10. Experimental transmission characteristics (P_{out}/P_{in}) of 3.781 meters of fiber#5 at the wavelength 1530 *nm* (circles). The solid line corresponds to the analytical transmission characteristics where P_{out} is calculated from equation (3.5) using the values of α_s, P_{in}, L, and P_{sat}.

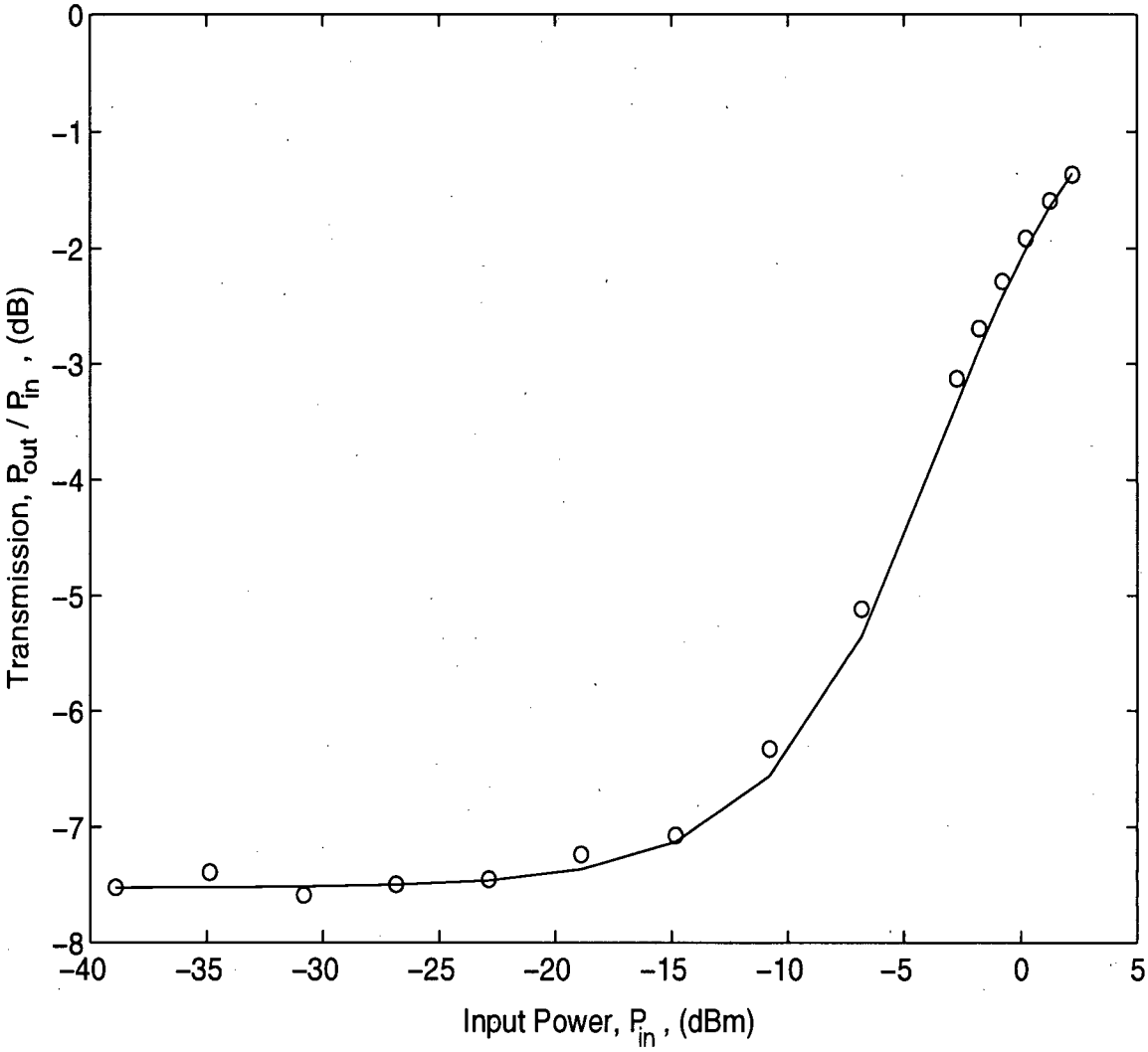

Figure 3.11. Experimental transmission characteristics (P_{out}/P_{in}) of 3.781 meters of fiber#5 at the wavelength 1550 *nm* (circles). The solid line corresponds to the analytical transmission characteristics where P_{out} is calculated from equation (3.5) using the values of α_s, P_{in}, L, and P_{sat}.

Summary of Chapter 3

In this chapter problems and difficulties associated with the conventional techniques for the measurement of the spectral fluorescence and the fluorescence lifetime have been described, as well as the new setups which were designed to simplify the measurement of these parameters. Also, experimental procedures for the measurement of other fiber parameters, such as spectral absorption coefficient, gain coefficient, and signal saturation power, have been described.

Chapter 4

Summary, Conclusions, and Recommendations for Future Work

4.1. Summary and Conclusions

The theory of operation of single-mode, erbium-doped fiber amplifiers pumped at 980 *nm* has been described. Details of the derivation of the general rate equation for the propagation of signal, pump, and spontaneous emission has been provided. Based on this rate equation and McCumber's theory of phonon-terminated optical masers, a closed form expression relating the fluorescence spectra of a single-mode erbium-doped fiber to its spectral absorption coefficient has been derived. Accordingly, a rigorous basis for the assessment of the applicability of McCumber's theory to the study of ${}^4I_{13/2} \Leftrightarrow {}^4I_{15/2}$ transitions in erbium-doped fibers has been established. For the cases of five silica-based, erbium-doped fibers, experimental results were used to validate this closed form expression and, thereby, the applicability of McCumber's theory to the study of ${}^4I_{13/2} \Leftrightarrow {}^4I_{15/2}$ transitions in silica-based, erbium-doped fibers.

Previous attempts, made by several researchers, to determine the absorption and emission cross-sections of erbium-doped fibers have been described, and the reasons for their lack of success with regard to the accurate evaluation of these parameters have been explained. Building upon the application of McCumber's theory to the general rate equation for the propagation of signal, pump, and amplified spontaneous emission, an analytical expression has been

derived by which the absorption and emission cross-sections can be conveniently and accurately determined using the easily measured spectral absorption coefficient, the gain coefficient at one particular wavelength, and the fluorescence lifetime. Experiments were performed to evaluate the spectral cross-sections of an erbium-doped fiber over the wavelength range 1400-1650 *nm*, and the accuracy of the calculated cross-sections was ensured by comparing the measured values of saturation powers at 1530 *nm* and 1550 *nm* with the ones calculated using the values of the cross-sections.

Existing difficulties with regard to the accurate estimation of the erbium ion concentration inside fiber cores have been described, and an analytical method for its simple determination has been proposed.

Problems and difficulties associated with the conventional techniques for the measurement of the spectral fluorescence and the fluorescence lifetime have been described, and new setups were designed to simplify the measurement of these parameters. Also, experimental procedures for the measurement of other fiber parameters, such as spectral absorption coefficient, gain coefficient, and signal saturation power, have been described.

In conclusion our new techniques for the determination of absorption and emission cross-sections, erbium ion concentration inside the fiber core, evaluation of the normalized fluorescence spectra from the spectral absorption coefficient, and measurement of the spectral fluorescence and fluorescence lifetime, can provide a much simpler and potentially more accurate means for characterizing erbium-doped fibers. This directly upgrades the accuracy of the numerical models commonly used for predicting the behavior and optimizing the performance of erbium-doped fiber amplifiers.

4.2. Recommendation for future research

As a first step towards continuing the work presented in this thesis, determination of the shape of the erbium distribution inside the fiber core using a recently proposed technique by D. Uttamchandani *et. al.* [21] is recommended. Once the erbium distribution is known the erbium ion concentration can be simply calculated from equation (2.22) by using the easily measured spectral absorption coefficient, gain coefficient at one particular wavelength, and the fluorescence lifetime. Subsequently, by knowing the values of the above parameters, together with the fiber absorption coefficient at the pump wavelength, the other fiber parameters, such as spectral absorption and emission cross-sections, signal saturation powers, pump saturation power, and absorption cross-section at the pump wavelength, can be simply calculated. In this way erbium-doped fibers can be completely characterized. Using the values of erbium-doped fiber parameters, the general rate equations for EDFAs can be solved, and important characteristics of EDFAs such as gain, and noise figure can be calculated.

References

[1] D. Baldwin, T. Eppes, J. Holland, H. Kuehler, and P. Steensma, "Optical Fiber Transmission System Demonstration Over 32 Km With Repeaters Data Rate Transparent Up to 2.3 Mbits/s," *IEEE Trans. Comm.,* vol. COM-26, no. 7, p. 1045, 1978.

[2] K. Monham, R. Plastow, A. Carter, and R. Goodfellow, "1.3 Gbit/s Transmission over 107 Km of Dispersion-Shifted Monomode Fiber Using a 1.55μm Multimode Laser," *Electron. Lett.,* vol. 21, no. 14, p. 619, 1985.

[3] S. Poole, D. Payne, and M. Fermann, "Fabrication of Low-Loss Optical Fibers Containing Rare-Earth Ions," *Electron. Lett.,* vol. 21, no. 17, p. 737, 1985.

[4] R. Mears, L. Reekie, I. Jauncy, and D. Payne, "High Gain Rare-Earth-Doped Fiber Amplifier Operating at 1.54 μm," *Optical Fiber Communications OFC'87,* Washington, D.C., Proc. vol. 3, p. 167, 1987.

[5] N. Bergano, J. Aspell, C. Davidson, P. Trischitta, B. Nyman, F. Kerfoot, "Bit Error Rate Measurements of 14000 Km 5 Gbit/s Fiber-Amplifier Transmission System Using Circulating Loop," *Electron. Lett.,* vol. 27, no. 21, p. 1889, 1991.

[6] A. Gnauck, B. Kasper, R. Linke, R. Dawson, T. Koch, T. Bridges, E. Burkhardt, R. Yen, D. Wilt, J. Campbell, K. Nelson, and L. Cohen, "4-Gbit/s Transmission over 103 Km of Optical Fiber Using a Novel Electronic Multiplexer/Demultiplexer," *IEEE J. Lightwave Technol.,* vol LT-3, no. 5, p.1032, 1985.

[7] A. Bjarklev, *"Optical Fiber Amplifiers: Design and System Applications,"* Artech House, Boston, MA, 1993.

[8] E. Desurvire, "Erbium-Doped Fiber Amplifiers," John Wiley & Sons, New York, 1994.

[9] E. Desurvire, J. Simpson, and P. Becker, "High-gain erbium-doped travelling-wave fiber amplifier," *Optics Lett.,* vol. 12, no. 11, p. 888, 1987.

[10] J. Armitage, "Three-level fiber laser amplifier: a theoretical model," *Applied Optics,* vol. 27, no. 23, p. 4831, 1988.

[11] P. Morkel, and R. Laming, "Theoretical modeling of erbium-doped fiber amplifiers with excited state absorption," *Optics Lett.,* vol. 14, no. 19, p. 1062, 1989.

[12] E. Desurvire, "Analysis of noise figure spectral distribution in erbium-doped fiber ampli-

fiers pumped near 980 and 1480 nm," *Applied Optics,* vol. 29, no. 21, p. 3118, 1990.

[13] M. Peroni and M. Tamburrini, "Gain in erbium-doped fiber amplifiers: a simple analytical solution for the rate equations," *Optics Lett.,* vol. 15, no. 15, p. 842, 1990.

[14] B. Pedersen, K. Dybdal, C.D. Hansen, A. Bjarklev, J. Povlsen, H. Pommer, and C. Larsen, "Detailed theoretical and experimental investigation of high-gain erbium-doped fiber amplifier," *IEEE Photonics Technol. Lett.,* vol. 2, no. 12, p. 863, 1990.

[15] C. Giles and E. Desurvire, "Modeling Erbium Doped Fiber Amplifiers," *IEEE J. Lightwave Technol.,* vol. 9, no. 2, 1991.

[16] T. Pfeiffer and H. Bulow, "Analytical Gain Equation for Erbium-Doped Fiber Amplifiers Including Mode Profiles and Dopant Distribution," *IEEE Photonics Technol. Lett.,* vol. 4, no. 5, p. 449, 1992.

[17] F. Ruhl, "Accurate Analytical Formulas for Gain-Optimized EDFAs," *Electron. Lett.,* vol. 28, no. 3, p. 312, 1992.

[18] K. Bertilsson, P. Andrekson, and B. Olsson, "Noise Figure of Erbium Doped Fiber Amplifiers in the Saturated Regime," *IEEE Photonics Technol. Lett.,* vol. 6, no. 2, p. 199, 1994.

[19] W. Miniscalco and R. Quimby, "General procedure for the analysis of Er^{3+} Cross Sections," *Optics Lett.,* vol. 16, no. 4, p. 258, 1991.

[20] H. Zech, "Measurement Technique for the Quotient of Cross Sections $\sigma_e(\lambda_s)/\sigma_a(\lambda_s)$ of Erbium Doped Fibers," *IEEE Photonics Technol. Lett.,* vol. 7, no. 9, p. 986, 1995.

[21] D.Uttamchandani, A. Othonos, A. Alavie, and M. Hubert, "Determination of Erbium Distribution in Optical Fibers Using Confocal Optical Microscopy," *IEEE Photonics Technol. Lett.,* vol. 6, no. 3, p. 437, 1994.

[22] NOI Bulletin, "Optical Fiber Fabrication Lab," vol. 1, no. 1, 1990.

[23] J. Sandoe, P. Sarkies, and S. Parke, "Variation of Er^{3+} cross-section for stimulated emission with glass composition," *J. Phys. D: Appl. Phys.,* vol. 5, p. 1788, 1972.

[24] W. Barnes, R. Laming, E. Tarbox, and P. Morkel, "Absorption and Emission Cross Section of Erbium Doped Silica Fibers," *IEEE J. Quantum. Electron.,* vol. 27, no. 4, p. 1004, 1991.

[25] S. Zemon, G. Lambert, L. Andrews, W. Miniscalco, B. Hall, T. Wei, and R. Folweiler,

"Characterization of Er^{3+}-doped glasses by fluorescence line narrowing," *J. Applied Phys.*, May 1991.

[26] R. Quimby and W. Miniscalco, "Determination of stimulated emission cross section for erbium-doped glass," *OSA 1990 Annual Metting,* Paper MCC2, 1990.

[27] D. McCumber, "Theory of phonon-terminated optical masers," *Phys. Rev.,* vol. 134, p. A299, 1964.

[28] M. Singh, D. Oblas, J. Reese, W. Miniscalco, and T. Wei, "Measurement of the Spectral Dependence of Absorption Cross Section for Erbium-Doped Single-Mode Optical Fiber," *Symposium on Optical Fiber Measurements*, Boulder, 1990. (NIST special Publ. no. 792, p. 93)

[29] S. Poole, D. Payne, R. Mears, M. Fermann, and R. Laming, "Fabrication and Characterization of Low-loss Optical Fibers Containig Rare-Earth Ions," *IEEE J. Lightwave Technol.,* vol. 4, no.7, p. 870, 1986.

[30] J. Simpson and J. MacChesney, "Alternate Dopants for Silica Waveguides," *Optical Fiber Communications OFC'82,* paper TuCc5, 1982.

[31] H. Suda, S. Shibata, and M. Nakahara, "Double-Flame VAD process for High-Rate Optical Preform Fabrication," *Electron Lett.,* vol. 21, no. 1, p. 29, 1985.

[32] P. Bocko, "Rare-Earth Doped Optical Fibers by the Outside Vapour Deposition Process," *Optical Fiber Communications OFC'89,* Houston, paper TuG2, 1989.

[33] J. Townsend, S. Poole, and D. Payne, "Solution-Doping Technique for Fabrication of Rare-Earth-Doped Optical Fibers," *Electron Lett.,* vol. 23, no. 7, p. 329-331, 1987.

[34] B. Ainslie, J. Armitage, S. Craig, and B. Wakefield, "Fabrication and Optimization of Erbium Distribution in Silica Based Doped Fibers," Proc. of *14th European Conference on Optical Communications ECOC'88,* Brighton, p. 62, 1988.

[35] R. Reisfeld, "Radiative and non-radiative transitions of rare-earth ions in glass," in *Structure and Bonding,* no. 22, Springer-Verlag, New York.

[36] B. Saleh and M. Teich, "Fundamentals of Photonics," John Wiley & Sons, New York, 1991.

[37] R. Laming, M. Farries, P. Morkel, L. Reekie, D. Payne, P. Scrivener, F. Fontana, and A. Righetti, "Efficient pump wavelengths of erbium-doped fiber optical amplifier," *Electron Lett.,* vol. 25, no. 1, p. 12, 1989.

[38] M. Shimuzu, M. Yamada, M. Horiguchi, T. Takeshita, and M. Okayash, "Erbium-doped fiber amplifiers with an extremely high gain coefficient of 11.0 dB/mW," *Electron Lett.,* vol. 26, p. 1641, 1990.

[39] R. Laming and D. Payne, "Noise Characteristics of Erbium-Dope Fiber Amplifier with 54 dB Gain and 3.1 dB Noise Figure," *IEEE Photonics Technol. Lett.,* vol. 2, no. 6, p. 418, 1990.

[40] R. Laming, M. Zervas, and D. Payne, "Erbium-Doped Fiber Amplifier with 54 dB Gain and 3.1 dB Noise Figure," *IEEE Photonics Technol. Lett.,* vol. 4, no. 12, p. 1345, 1992.

[41] H. Zarem, J. Paslask, M. Mittlestein, J. Ungar, and I. Ury, "High power fiber coupled strained layer InGaAs lasers emitting at 980nm," in proc. *Topical Meeting of Optical Amplifiers and Applications,* Optical Society of America, paper pdp4, 1991.

[42] C. Layne, W. Lowdermilk, and M. Weber, "Multiphonon relaxation of rare-earth ions in oxide glasses," *Phys. Rev. B*, vol. 16, no. 1, p. 10, 1977.

[43] B. Ainslie, S. Craig, and S. Davey, "The Absorption and Fluorescence Spectra of Rare Earth Ions in Silica-Based Monomode Fiber," *IEEE J. Lightwave Technol.,* vol. 6, no. 2, p. 287, 1988.

[44] C. Giles, C. Burrus, D. Digiovani, N. Dutta, and G. Raybon, "Characterization of Erbium-Doped Fibers and Application to Modeling 980-nm and 1480-nm Pumped Amplifiers," *IEEE Photon. Tech. Lett,* vol. 3, p. 363, 1991.

[45] M. Spiegel, "*Mathematical Handbook of Formulas and Tables,*" McCraw-Hill Book Company, New York, 1968.

[46] E. Desurvire, J. Zyskind, and C. Giles, "Design Optimization for Efficient Erbium-Doped Fiber Amplifiers," *IEEE J. Lightwave Technol.,* vol. 8, no. 11, p. 1730, 1990.

[47] D. Gloge, "Weakly guiding fibers," *Applied Optics*, vol. 10, no. 10, 1152, 1971.

[48] W. Etten and J. Plaats, "*Fundamentals of Optical Fiber Communications,*" Prentice Hall, UK, 1991.

[49] A. Saleh, R. Jopson, J. Evankow, and J. Aspell, "Modeling of Gain in Erbium-Doped Fiber Amplifiers," *IEEE Photon. Tech. Lett,* vol. 2, no. 10, p. 714, 1991.

[50] M. Ohashi, "Design Considerations for an Er^{3+}-Doped Fiber Amplifier," *IEEE J. Lightwave Technol.,* vol 9, no. 9, p. 1099, 1991.

[51] D. Oblas, F. Pink, M. Singh, J. Connolly, D. Dugger, and T. Wei, *Digest of Materials Research Society Annual Meeting 1992,* (MRS Pittsburgh, pa), paper J6.3., 1992.

[52] P. France, "*Optical Fibre Lasers and Amplifiers*", Blackie, Florida, 1991.

[53] S. Poole, D. Payne, R. Mears, M. Fermann, and R. Laming, "Fabrication and Characterization of Low-Loss Optical Fibers Containing Rare-Earth Ions," *IEEE J. Lightwave Technol.,* vol 4, No. 7, p. 870, 1986.

[54] B. Ainsile, "A Review of the Fabrication and Properties of Erbium-Doped Fibers for Optical Amplifiers," *IEEE J. Lightwave Technol.,* vol 9, no. 2,1991.

[55] D. Marcuse, "Principles of Optical Fiber Measurements," Academic Press, New York, 1981.

[56] C. Hentschel, E. Muller, and E. Leckel, "EDFA Noise Figure Measurements," 1994 lightwave symposium, Hewlett-Packard Company, 1994.

[57] H. Bulow and T. Pfeiffer, "Calculation of the Noise Figure of Erbium-Doped Fiber Amplifiers Using Small Signal Attenuations and Saturation Powers," *IEEE Photon. Tech. Lett,* vol. 4, No. 12, p. 1351, 1992.

[58] A. Siegman, "*Lasers*", University Science Books, Mill Valley, CA, 1986.

[59] C. Layne, W. Lowdermilk, and M. Weber, "Nonradiative relaxation of rare earth ions in silicate laser glass," *IEEE J. Quantum Electron.,* vol. 11, p. 798, 1975.

[60] K. Gschneider and L. Eyring, "*Handbook on the physics and chemistry of rare-earths,*" Elsevier Science Publishers, 1987.

[61] A. Yariv, "*Quantum Electronics*", Second Edition, John Wiley & Sons, New York, 1975.

[62] R. Macfarlane and R. Shelby, "Homogeneous line broadening of optical transitions of ions and molecules in glasses" *Journal of Luminescence*, vol. 36, p. 179, 1987.

[63] H. Kogelnick and A. Yariv, "Considerations of noise and schemes for its reduction in laser amplifiers," *proc. IEEE*, p. 165, 1964.

[64] E. Desurvire and J. Simpson, "Amplification of Spontaneous Emission in Erbium-Doped Single-Mode Fiber," *IEEE J. Lightwave Technol.,* vol. 7, no. 5, p. 835, 1989.

[65] E. Desurvire, "Study of the complex atomic susceptibility of erbium-doped fiber ampli-

fiers," *IEEE J. Lightwave Technol.,* vol. 8, no. 10, p. 1517, 1990.

[66] W. Miniscalco, "Erbium-Doped Glasses for Fiber Amplifiers at 1500nm," *IEEE J. Lightwave Technol.,* vol. 9, no. 2, p. 234, 1991.

[67] W. Miniscalco, L. Andrews, B. Thompson, T. Wei, and B. Hall, "$^4I_{13/2} \leftrightarrow {}^4I_{15/2}$ emission and absorption cross sections for Er^{3+} doped glasses," in *Tunable Solid State Lasers,* OSA Proc. Series, vol. 5, p. 354, 1989.

[68] P. Milonni and J. Eberly, "*Lasers*", John Wiley, New York, 1988.

[69] W. F. Krupke, "Radiative transition probabilities within the $4f^3$ ground configuration of Nd:YAG," *IEEE J. Quantum Electron*, vol. 7, no. 4, p. 153, 1971.

[70] E. Desurvire and J. Simpson, "Evaluation of $^4I_{15/2}$ and $^4I_{13/2}$ Stark-level energies in erbium-doped alumino silicate glass fiber," *Optics Lett.,* vol. 15, p. 547, 1990.

[71] W. Barnes, R. Laming, P. Morkel, and E. Tarbox, "Absorption-emission cross-section ratio for Er^{3+}-doped fibers at $1.55\mu m$," in Proc. *Conference on Lasers and Electro-Optics,* CLEO' 90, paper JTUA3, p. 50, Optical Society of America, Washington DC, 1990.

[72] K. Dyhal, N. Bjerre, J. Pederson, and C. Larsen, "Spectroscopic properties of erbium-doped silica fibers and preforms," in proc. *SPIE Conference on Fiber Laser Sources and Amplifiers,* vol, 1171, p. 209, 1989.

[73] MATLAB User's Guide for Unix Workstations, The Math Works, Inc., Natick, Mass, 1992.

Appendix A: Rate equation analysis of the erbium ion population

As was discussed in section 2.2, by choosing the 980 *nm* pump band, only the first three energy levels of erbium need to be considered. Here, in accordance with the literature, a three level rate equation model, which has been traditionally used for some lasers [58] (e.g., a Ruby laser), is adapted for modeling light amplification in erbium doped, single mode fibers. Figure A.1 shows these three levels as well as all of the possible transitions between them. Here R is the absorption rate from level 1 to 3, corresponding to the 980 *nm* pump absorption. W_{12} and W_{21} are, respectively, the absorption rate and the stimulated emission rate between levels 1 and 2 in the 1520-1570 *nm* signal band. A_{21} represents the spontaneous decay rate from level 2 to level 1. For the case of erbium-silica glass, experimental measurements have shown that the radiative quantum efficiency for the ${}^4I_{13/2} \rightarrow {}^4I_{15/2}$ transition is 99.93% [42], [59]. Therefore, A_{21} can be assumed to be only the radiative spontaneous decay rate, with $A_{21} = 1/\tau$, where τ, by definition, is the fluorescence lifetime [8]. A_{32} and A_{31} are the two possible decay rates, for ions, from the pump level. Experimental studies for the case of erbium-silica glass have shown that the ${}^4I_{11/2} \rightarrow {}^4I_{13/2}$ transition is essentially nonradiative, with a rate of $5.53 \times 10^4\ s^{-1}$. Furthermore, the total decay rates of A_{31} + radiative decay rate of $A_{32} \approx 125\ s^{-1}$ [60]. As a result we can ignore the decay rate A_{31}, and we can also assume that the transitions corresponding to the decay rate A_{32} are totally nonradiative.

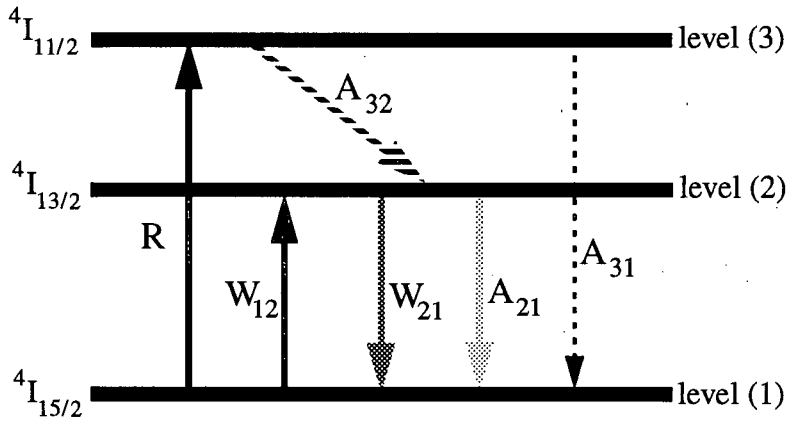

Figure A.1. Energy level diagram corresponding to the first three levels of erbium ions in the glass host, and all of the possible transitions between these levels.

Now, we can write the rate equations corresponding to the population concentrations of erbium ions in the ground level N_1, metastable level N_2, and pump level N_3 as [8]:

$$\frac{dN_1}{dt} = -RN_1 - W_{12}N_1 + W_{21}N_2 + A_{21}N_2 \ , \tag{A.1}$$

$$\frac{dN_2}{dt} = W_{12}N_1 - W_{21}N_2 - A_{21}N_2 + A_{32}N_3 \ , \tag{A.2}$$

$$\frac{dN_3}{dt} = RN_1 - A_{32}N_3 \ . \tag{A.3}$$

If we consider the steady state regime of operation, i.e., $\frac{dN_i}{dt} = 0 \ \ (i = 1, 2, 3)$, as well as the fact that $A_{32} \gg R$ [8], then the population density of ions in the three levels can be written as:

$$N_1 = \rho \frac{1 + W_{21}\tau}{1 + (R + W_{12} + W_{21})\tau} , \tag{A.4}$$

$$N_2 = \rho \frac{(R + W_{12})\tau}{1 + (R + W_{12} + W_{21})\tau} , \tag{A.5}$$

and

$$N_3 = \frac{R}{A_{32}} N_1 \approx 0 , \tag{A.6}$$

where $\rho = N_1 + N_2 + N_3$ is the erbium ion density. Equation (A.6) shows that the pump level population, N_3, is approximately zero. This is due to the fast nonradiative decay rate of ions from the pump level to the metastable level (A_{32}).

While, in the above analysis, each energy level is assumed to be nondegenerate, in reality such is not the case, and, as was mentioned in section 2.2, due to the Stark effect, each single energy level of the erbium splits into a manifold of g energy sublevels, where g is the total level degeneracy. Nevertheless, through a more complex rate equation model [8], it is shown that the nondegenerate assumption, of the main energy levels of erbium in glass hosts, still remains accurate. This is because of the fast thermalization effect which prevails within the Stark manifolds. The thermalization effect maintains a constant population distribution within the manifolds (Boltzman's distribution), which eventually makes it possible to consider each manifold as a single energy level.

Appendix B: General rate equation for the propagation of signal, pump, and amplified spontaneous emission in single mode erbium doped fibers.

In Appendix A the steady state populations of erbium ions in the first three energy levels were shown. Now, here, by considering the effect of light confinement in an erbium doped, single mode fiber, and relating the fiber waveguide parameters to the transition rates of erbium ions between the three levels, a general rate equation for the propagation of signal, pump, and amplified spontaneous emission will be derived.

When a light signal at wavelength λ with intensity I_s (power per area) passes through an active medium of length dz, and atomic population densities of N_1, for the ground level, and N_2, for the metastable level, the intensity change dI_s is given by [8], [61]:

$$dI_s = (\sigma_e(\lambda)N_2 - \sigma_a(\lambda)N_1)\, I_s\, dz\,, \tag{B.1}$$

where $\sigma_e(\lambda)$ is the emission cross section and $\sigma_a(\lambda)$ is the absorption cross section, both at the signal wavelength λ. Now we consider the fact that the signal light is actually guided in a single mode fiber. If the signal power coupled into the mode is $P_s(\lambda)$, and the mode power distribution at λ is $\psi_s(\lambda, r, \theta)$, then the light intensity distribution, $I_s(\lambda, r, \theta)$, in the fiber transverse plane is given as [8],

$$I_s(\lambda, r, \theta) = P_s(\lambda)\, \frac{\psi_s(\lambda, r, \theta)}{\int_S \psi_s(\lambda, r, \theta) r\, dr\, d\theta}\,, \tag{B.2}$$

where r is the radial coordinate, θ is the azimutal coordinate, and S denotes that the integral should be taken over the entire transverse plane.

From equations (B.1) and (B.2), we can write:

$$\frac{dP_s(\lambda)}{dz} = P_s(\lambda) \int_S \{\sigma_e(\lambda)N_2(\lambda, r, \theta) - \sigma_a(\lambda)N_1(\lambda, r, \theta)\}\overline{\psi}_s(\lambda, r, \theta) r dr d\theta \ , \qquad \text{(B.3)}$$

where $\overline{\psi}_s$ is the normalized mode power at wavelength λ defined as:

$$\overline{\psi}_s(\lambda, r, \theta) = \frac{\psi_s(\lambda, r, \theta)}{\int_S \psi_s(\lambda, r, \theta) r dr d\theta} \ . \qquad \text{(B.4)}$$

Equation (B.3) represents the rate of signal power change, as light propagates through the fiber in the guided mode. In deriving the above rate equation, equation (B.3), it is assumed that all of the erbium ions present in the active medium at any point (z, r, θ) have identical cross sections. This is equivalent to assuming homogeneous broadening, i.e., every ion in the collection of ions has the same center frequency and the same lineshape and frequency response, so that a signal applied to the transition has exactly the same effect on all the ions in the collection [58]. In reality, such is not the case for laser systems in which the levels are split by the Stark effect. This is because the lower and upper energy levels are split into manifolds of g_1 and g_2 sublevels. Therefore, the laser line corresponding to the two main levels, are made of the superposition of $g_1 \times g_2$ possible laser transitions, where each laser transition between the two Stark manifolds has a different characteristic. Furthermore, variation of the crystalline electric field from site to site in the glass host causes a nonuniform Stark splitting effect. These effects induce inhomogeneous broadening of the laser line. However, in silica based erbium doped fibers the Stark sublevels have small energy gaps and therefore are strongly

coupled by the effect of thermalization [8], [62]. For the case of erbium-silica, the thermalization rates A_{NR}^{+} and A_{NR}^{-}, which correspond to upward excitation (absorption) and downward nonradiative relaxation (creation of a phonon) of ions between the Stark sublevels respectively, are on the order of $1ps$ or less [8]. Since these thermalization rates generally overtake the pumping and stimulated emission rates, the condition of thermal equilibrium within the Stark manifolds is always maintained [8]. Therefore, since the relative populations within the Stark manifolds are unchanged by pumping or saturation, the spectral characteristics of ${}^4I_{13/2} \Leftrightarrow {}^4I_{15/2}$ transition cross sections also remain unchanged. As a result the homogeneous broadening approximation, made in the derivation of equation (B.3) for the case of commonly used silica based erbium doped fibers, is justifiable.

In order to derive a general rate equation for the signal, the effect of amplified spontaneous emission (ASE) also has to be taken into account [8]. The generation of ASE is an effect of radiative spontaneous deexcitation of the erbium ions from the metastable level. The photons arising from this process have no coherence characteristics with respect to the incoming signal light. The generated photons are then multiplied as they travel along the amplifier, creating background noise which is added to the signal light. This background noise is called the amplified spontaneous emission. The rate of creation of spontaneous emission power coupled into the fiber mode, and in the direction of the incoming signal (here the positive z direction) in the frequency interval between ν and $\nu + \Delta\nu$ ($\Delta\nu$ represents a frequency slot of arbitrary width) is given by [8], [63], [64]:

$$\frac{dP_{SE}(\nu)}{dz} = 2P_0(\nu)\sigma_e(\nu)\int_S N_2(\nu, r, \theta)\overline{\psi}_s(\nu, r, \theta)rdrd\theta \ , \qquad \text{(B.5)}$$

where $P_0(\nu) = h\nu\Delta\nu$ is defined as the equivalent input noise power corresponding to one photon per mode in a bandwidth of $\Delta\nu$. Using the relation $|\Delta\nu| = |c\Delta\lambda / \lambda^2|$, we can write $P_0(\lambda) = hc^2\Delta\lambda / \lambda^3$.

Now, using equations (B.3) and (B.5) we can express the evolution of the total signal power, including the effect of added ASE, at wavelength λ and in the wavelength interval $\Delta\lambda$, by:

$$\frac{dP_t(\lambda)}{dz} = \int_S \{\sigma_e(\lambda)N_2(\lambda, r, \theta)[P_s(\lambda) + 2P_0(\lambda)] - \sigma_a(\lambda)N_1(\lambda, r, \theta)P_s(\lambda)\}\overline{\psi}_s(\lambda, r, \theta)rdrd\theta \ , \qquad \text{(B.6)}$$

where $P_t(\lambda) = P_s(\lambda) + P_{SE}(\lambda)$.

By using the radial symmetry property of the fundamental mode in the fiber, and also assuming radial symmetry for the erbium density distribution inside the fiber core, equation (B.6) can be simplified as:

$$\frac{dP_t(\lambda)}{dz} = 2\pi\int_0^\infty \{\sigma_e(\lambda)N_2(\lambda, r)[P_s(\lambda) + 2P_0(\lambda)] - \sigma_a(\lambda)N_1(\lambda, r)P_s(\lambda)\}\overline{\psi}_s(\lambda, r)rdr \ . \qquad \text{(B.7)}$$

Equation (B.7) is expressed in terms of steady state atomic populations N_1 and N_2, which cannot be determined experimentally. In the following procedure these population densities

will be related to the experimentally measurable signal and pump powers coupled into the fiber mode.

For the case of single mode fibers, a mode power radius ω_s, corresponding to the mode power distribution ψ_s, can be defined through [65],

$$\omega_s(\lambda) = \left(\frac{1}{\pi}\int_S \psi_s(\lambda, r, \theta) r dr d\theta\right)^{\frac{1}{2}} . \tag{B.8}$$

By using the radial symmetry of the fundamental mode, we can write:

$$\omega_s(\lambda) = \left(2\int_0^{\infty} \psi_s(\lambda, r) r dr\right)^{\frac{1}{2}} , \tag{B.9}$$

where it is assumed that $\psi_s(\lambda, r=0) = 1$. Therefore, equation (B.4) can be written as:

$$\bar{\psi}_s(\lambda, r) = \frac{\psi_s(\lambda, r)}{\pi\ \omega_s^2(\lambda)} . \tag{B.10}$$

Now, from equations (B.2) and (B.10), the signal intensity at fiber coordinate z and distance r from the core axis, $I_s(\lambda, r, z)$, can be written as:

$$I_s(\lambda, r, z) = \frac{P_s(\lambda, z)\psi_s(\lambda, r)}{\pi\ \omega_s^2(\lambda)} , \tag{B.11}$$

where $P_s(\lambda, z)$ is the signal power at wavelength λ coupled into the fiber mode.

The proportionality between $I_s(\lambda, r, z)$ and the stimulated emission rate $W_{21}(\lambda, r, z)$ is given by [8], [61]:

$$W_{21}(\lambda, r, z) = \frac{\lambda^3}{8\pi n^2 h c \tau} I_s(\lambda, r, z)\xi(\lambda) \ , \tag{B.12}$$

where h is Plank's constant, n is the refractive index of the fiber core, and $\xi(\lambda)$ is the line-shape function defined as:

$$\xi(\lambda) = \frac{8\pi n^2 \tau \sigma_e(\lambda)}{\lambda^2} \ . \tag{B.13}$$

From equations (B.11)-(B.13) we can write:

$$W_{21}(\lambda, r, z) = \frac{\lambda \psi_s(\lambda, r) \sigma_e(\lambda)}{\pi h c \omega_s^2(\lambda)} P_s(\lambda, z) \ . \tag{B.14}$$

Using the relationship $W_{21} = \frac{\sigma_e}{\sigma_a} W_{12}$ [8], and equation (B.14) we can also write:

$$W_{12}(\lambda, r, z) = \frac{\lambda \psi_s(\lambda, r) \sigma_a(\lambda)}{\pi h c \omega_s^2(\lambda)} P_s(\lambda, z) \ . \tag{B.15}$$

Likewise, for the pumping rate $R(\lambda_p, r, z)$ a definition similar to equation (B.15) can be introduced [8]:

$$R(\lambda_p, r, z) = \frac{\lambda_p \psi_p(\lambda_p, r) \sigma_a(\lambda_p)}{\pi h c \omega_p^2(\lambda_p)} P_p(\lambda_p, z) \ , \tag{B.16}$$

where $\sigma_a(\lambda_p)$ is the pump absorption cross section at wavelength λ_p, $P_p(\lambda_p, z)$ is the pump power at wavelength λ_p coupled into the fundamental fiber mode, $\psi_p(r)$ the mode power distribution at wavelength λ_p, and ω_p is the mode power radius at frequency λ_p defined similarly to equation (B.9).

The saturation power at signal wavelength λ is defined by [8]:

$$P_{sat}(\lambda) = \frac{hc\pi\omega_s^2(\lambda)}{[\sigma_a(\lambda)+\sigma_e(\lambda)]\lambda\tau} \quad . \tag{B.17}$$

Likewise, the saturation power at pump frequency, considering the fact that $\sigma_e(\lambda_p) = 0$ for 980 *nm* pumping, can be written as:

$$P_{sat}(\lambda_p) = \frac{hc\,\pi\,\omega_p^2(\lambda_p)}{\sigma_a(\lambda_p)\,\lambda_p\,\tau} \quad . \tag{B.18}$$

Using equations (B.14)-(B.18), we can write the steady state atomic populations N_1 and N_2 expressed in equations (A.4) and (A.5) as functions of optical signal and pump powers:

$$N_1(\lambda, r, z) = \rho(r)\,\frac{1 + \dfrac{\sigma_e(\lambda)\psi_s(\lambda, r)}{\sigma_e(\lambda)+\sigma_a(\lambda)} \cdot \dfrac{P_s(\lambda, z)}{P_{sat}(\lambda)}}{1 + \dfrac{P_p(\lambda_p, z)}{P_{sat}(\lambda_p)}\psi_p(\lambda_p, r) + \dfrac{P_s(\lambda, z)}{P_{sat}(\lambda)}\psi_s(\lambda, r)} \quad , \tag{B.19}$$

$$N_2(\lambda, r, z) = \rho(r)\,\frac{\dfrac{P_p(\lambda_p, z)}{P_{sat}(\lambda_p)}\psi_p(\lambda_p, r) + \dfrac{\sigma_a(\lambda)\psi_s(\lambda, r)}{\sigma_e(\lambda)+\sigma_a(\lambda)} \cdot \dfrac{P_s(\lambda, z)}{P_{sat}(\lambda)}}{1 + \dfrac{P_p(\lambda_p, z)}{P_{sat}(\lambda_p)}\psi_p(\lambda_p, r) + \dfrac{P_s(\lambda, z)}{P_{sat}(\lambda)}\psi_s(\lambda, r)} \quad . \tag{B.20}$$

Hence, the general rate equation for the propagation of signal, pump, and ASE (equation (B.7)) combined with equations (B.10),(B.19), and (B.20) takes the form:

$$\frac{dP_t(\lambda, z)}{dz} = \frac{2}{\omega_s^2(\lambda)} \int_0^\infty \rho(r)\Big\{\sigma_e(\lambda)\frac{\zeta_1 + \zeta_2}{1 + \zeta_1 + \zeta_3}[P_s(\lambda, z) + 2P_0(\lambda)] - \sigma_a(\lambda)\frac{1 + \zeta_4}{1 + \zeta_1 + \zeta_3}P_s(\lambda, z)\Big\}\psi_s(\lambda, r)rdr \tag{B.21}$$

$$\zeta_1 = \psi_p(\lambda_p, r)\,\frac{P_p(\lambda_p, z)}{P_{sat}(\lambda_p)}$$

$$\zeta_2 = \frac{\sigma_a(\lambda)\psi_s(\lambda, r)}{\sigma_a(\lambda) + \sigma_e(\lambda)}\,\frac{P_s(\lambda, z)}{P_{sat}(\lambda)}$$

$$\zeta_3 = \psi_s(\lambda, r)\,\frac{P_s(\lambda, z)}{P_{sat}(\lambda)}$$

$$\zeta_4 = \frac{\sigma_e(\lambda)\psi_s(\lambda, r)}{\sigma_a(\lambda) + \sigma_e(\lambda)}\,\frac{P_s(\lambda, z)}{P_{sat}(\lambda)}$$

Appendix C: Previous attempts at the determination of cross sections

As can be inferred from the general rate equation for the propagation of signal, pump, and ASE, equation (B.21), the gain and noise performance of the three level erbium doped fiber amplifiers are quite sensitive to the values of absorption and emission cross sections at signal wavelengths. Therefore, knowledge of these parameters is essential to modeling erbium doped fiber amplifiers for predicting signal gain and amplified spontaneous emission power. However, despite extensive efforts placed on the evaluation of cross sections by several researchers, relatively large uncertainty still exists throughout the literature regarding their actual values [19], [24], [28], [66], [67].

One of the principal approaches for the determination of cross sections is based on the Futchbacher-Ladenberg (FL) relationships [23]. However, several researchers have reported its failure for the ${}^4I_{13/2} \Leftrightarrow {}^4I_{15/2}$ transitions in erbium-glasses [19], [24], [25].

Generalized to the case in which the lower level and upper level are split into multiple sublevels, the FL relations take the form [8],[44]:

$$\sigma_e(\lambda) = \frac{\lambda^4 F(\lambda)}{8\pi n^2 c \tau \int_{\text{band}} F(\lambda) d\lambda}, \tag{C.1}$$

$$\sigma_a(\lambda) = \frac{g_2}{g_1} \cdot \frac{\lambda^4 \alpha(\lambda)}{8\pi n^2 c \tau \int_{\text{band}} \alpha(\lambda) d\lambda}, \tag{C.2}$$

where $F(\lambda)$ is the spectral fluorescence over the ${}^4I_{13/2} \rightarrow {}^4I_{15/2}$ emission band, $\alpha(\lambda)$ is

the absorption spectrum over the ${}^4I_{13/2} \rightarrow {}^4I_{15/2}$ absorption band, g_1 is the degeneracy of the ground level, and g_2 is the degeneracy of the metastable level. The integrals in equations (C.1) and (C.2) are taken over the entire emission and absorption bands, respectively. The FL relations which are derived from Einstein's A and B coefficients [68] can be applied only to cases where the populations of all the Stark sublevels are equal [69]. This condition is met only when the total Stark splitting energy, ΔE, is less than $k_B T$, where k_B is the Boltzman constant and T is the absolute temperature [8]. However, experimental evidence shows that the Stark splitting for the ${}^4I_{15/2}$ and ${}^4I_{13/2}$ states of erbium doped glasses are typically 300-400 cm^{-1} [25], [70], nearly twice $k_B T \approx 200\ cm^{-1}$ at room temperature; this suggests that the FL relations are inaccurate to some extent [8]. The inaccuracy of the FL relations was actually confirmed experimentally, [11], [19], [24], [71], as it was found that the measured peak cross sections $\eta^{peak} = \sigma_e(\lambda_{peak})/\sigma_a(\lambda_{peak}) = 0.84 - 0.94$, while the FL relations predicts values of $\eta^{peak} = 1.17 - 1.28$. For the case of commonly used Alumino-Phosphorous-silica fibers (Al/P -silica fiber) this discrepancy is estimated to be even greater than 50% [19]. Finally, in view of the above results, the Fuchtbauer-Ladenberg approach to the determination of the cross sections of ${}^4I_{13/2} \Leftrightarrow {}^4I_{15/2}$ transitions in erbium-glass looks flawed.

Alternatively, in 1991 Miniscalco and Quimby [19], [26], suggested that McCumber's theory of phonon terminated optical masers [27] could be used to determine either the absorption or emission cross sections if the other is known. In the first step they argued that McCumber's theory, in which a simple model is used to describe the operating properties of the insulating crystals doped with impurities, is appropriate for the study of the ${}^4I_{13/2} \Leftrightarrow {}^4I_{15/2}$ transitions of erbium doped glasses. In the model used in McCumber's theory, the energy levels of the

impurity ions are grouped into two manifolds, where each manifold is split into multiple sub-levels; this is identical to the ${}^4I_{15/2}$ and ${}^4I_{13/2}$ levels of erbium in a glass host. Furthermore, it is assumed that the nonradiative transition rate between the two manifolds is negligible compared with the radiative transition rate, and the time required to establish a thermal equilibrium within each manifold is very short compared to the spontaneous emission lifetime (spontaneous emission lifetime = 1 / radiative transition rate). These assumptions are satisfied for the case of erbium-glass, as the ${}^4I_{13/2} \rightarrow {}^4I_{15/2}$ transition is essentially radiative and the fluorescence lifetime of the metastable level is very long (around 10 *ms*). Accordingly, they concluded that McCumber's two level model is, in fact, ideally appropriate for the study of ${}^4I_{15/2}$ and ${}^4I_{13/2}$ levels of erbium in glass hosts. In the next step, based on McCumber's theory, they attempted to determine the values of emission cross sections for several types of erbium doped fibers. In their approach, the absorption cross section $\sigma_a(\lambda)$ was determined from measurements of the absorption coefficient, the erbium density distribution, and the optical mode field power distribution [28]. The emission cross section was then calculated from the measured absorption cross section using the McCumber relation given by [19],[27]:

$$\sigma_e(\lambda) = \sigma_a(\lambda) \exp\left(\frac{\varepsilon - \frac{hc}{\lambda}}{k_B T}\right), \tag{C.3}$$

where ε is the net free energy required to excite one erbium ion from the ${}^4I_{15/2}$ level to ${}^4I_{13/2}$ at temperature T. This parameter is defined by [19],[27]:

$$\varepsilon = k_B T \ln\frac{N_1}{N_2}, \tag{C.4}$$

where N_1/N_2 is the equilibrium population ratio between the two levels at temperature T in the absence of optical pumping. If the Stark sublevel energies in the ground level are labeled E_{1m} $(m = 1, \ldots, g_1)$ and in the metastable level are labeled E_{2n} $(n = 1, \ldots, g_2)$, for the case of erbium ions where $g_1 = 8$ and $g_2 = 7$, ε can be calculated according to [8],[19]:

$$\varepsilon = k_B T \ln\left(\frac{1 + \sum_{m=2}^{8} \exp\left(\frac{-\Delta E_{1m}}{k_B T}\right)}{\exp\left(\frac{-\Delta E_{21}}{k_B T}\right)\left[1 + \sum_{n=2}^{7} \exp\left(\frac{-\Delta E_{2n}}{k_B T}\right)\right]}\right) \tag{C.5}$$

where ΔE_{21} is the separation between the lowest component of each manifold, and ΔE_{1m}, ΔE_{2n} are the energy differences between Stark sublevels with respect to the lowest energy level in the corresponding manifold.

The evaluation of Stark sublevel energies is very difficult and often inaccurate. In addition, generally the positions of all the Stark sublevels are not known [19],[70]. This induces inaccuracy in the calculation of ε, and consequently the emission cross section. For the case of an Al/P-silica fiber the discrepancy between the measured peak value of the emission cross section and that calculated from equation (C.3) from the measured absorption cross section, and using an estimated value for the ε, was 28% [19]. This discrepancy for the other types of glasses varies from 1.4% for a fluorophosphate glass to 16% for a silicate glass [19]. In cases where ε was not known, they measured the absorption cross sections over the whole spectral absorption band. The measured absorption cross sections were then transformed into relative emission cross section spectra using equation (C.3). To obtain the absolute emission cross section, this relative spectra were then scaled by using the following expression from McCum-

ber's theory [19], [27]:

$$\frac{1}{\tau} = 8\pi c n^2 \int_{\text{band}} \frac{\sigma_e(\lambda)}{\lambda^4}\, d\lambda \ , \tag{C.6}$$

where τ is the fluorescence lifetime and n is the refractive index of the core.

In the above approach, although the requirement of evaluating ε is eliminated, there is still no guarantee that the calculated emission cross section spectrum is accurate. This could be attributed to errors introduced into the calculation from the uncertain values of the absorption cross sections. As was mentioned earlier, absorption cross sections have been determined based on the measured values of the erbium dopant concentration and its distribution within the fiber core [28]. Since the diameter of the actual fiber core is very small, this measurement is performed on slices of the fiber preform using secondary ion mass spectrometry (SIMS), where the accuracy of the measurement is estimated to be about 18% [28]. In addition to this error the final draw of the preform, into fiber, may create considerable changes in the erbium density distribution; this is attributable to changes in glass network structure that occur during preform collapse and fiberization, which are produced by various effects of phase transitions, codopant migration or diffusion, and erbium site rearrangements [72].

In order to assess the accuracy of the calculated cross sections using McCumber's theory, for several glasses, comparisons were made between the measured emission cross sections with that calculated from the absorption cross sections and the fluorescence lifetime using equation (C.6) [8], [19]. While excellent agreement was obtained over the wavelength range 1450-1650 nm, for the case of a fluorophosphate glass [19], large discrepancies (e.g., as much

as 13% to 25% in the wavelength range of 1520-1560 *nm*) were observed for the cases of several silica based erbium doped fibers [8]. Due to these rather large discrepancies, uncertainty still remains regarding the applicability of McCumber's theory for the study of ${}^4I_{13/2} \Leftrightarrow {}^4I_{15/2}$ transitions in erbium doped fibers.

In Section 2.3 of this thesis, a new approach is presented, by which the applicability of McCumber's theory to the study of silica based erbium doped fibers is validated.